

# **A simplified finite element model for assessing steel fibre reinforced concrete structural performance**

Ali A. Abbas BSc(Eng.), DIC, PhD, FHEA  
Senior Lecturer in Structural Engineering,  
School of Architecture, Computing and Engineering, University of East London,  
London E16 2RD, UK  
Tel.: 020 8223 6279, Fax: 020 8223 2963  
E-mail: abbas@uel.ac.uk

Sharifah M. Syed Mohsin BSc(Eng.), DIC, PhD  
Senior Lecturer,  
Faculty of Civil & Earth Resources, Universiti Malaysia Pahang,  
Lebuhraya Tun Razak, 26300 Gambang, Kuantang, Pahang, MALAYSIA  
E-mail:maszura@ump.edu.my

\* Demetrios M. Cotsovos Dipl Ing, MSc, DIC, PhD, CEng  
Lecturer in Structural Engineering,  
Institute of Infrastructure and Environment, School of the Built Environment, Heriot-Watt University,  
Edinburgh, EH14 4AS, UK,  
E-mail: D.Cotsovos@hw.ac.uk

\* Corresponding Author.

## **ABSTRACT**

*The present numerical investigation offers evidence concerning the validity and objectivity of the predictions of a simple, yet practical, finite element model concerning the responses of steel fibre reinforced concrete structural elements under static monotonic and cyclic loading. Emphasis is focused on realistically describing the fully brittle tensile behaviour of plain concrete and the contribution of steel fibres on the post-cracking behaviour it exhibits. The good correlation exhibited between the numerical predictions and their experimental counterparts reveals that, despite its simplicity, the subject model is capable of providing realistic predictions concerning the response of steel fibre reinforced concrete structural configurations exhibiting both ductile and brittle modes of failure without requiring recalibration.*

**Keywords:** steel fibres; concrete; finite-element analysis; cracking; numerical modelling; nonlinear behaviour

## 1. INTRODUCTION

A large number of finite-element (FE) models have been developed to date aiming to describe the nonlinear behaviour of reinforced concrete (RC) structural configurations under static and dynamic loading. The analytical formulation of such models is generally based on the combined use of [1,2]: (i) relevant experimental data and (ii) continuum mechanics theories (i.e. nonlinear elasticity, plasticity, visco-plasticity and damage mechanics). The latter formulation usually incorporates a number of parameters, the evaluation of which is essential for achieving close correlation between the numerically predicted nonlinear specimen behaviour and its experimentally-established counterpart. These parameters are usually associated with post-failure concrete behaviour (i.e. strain softening, tension stiffening, shear-retention ability) and their values are often established through calibration based on the use of experimental information at the structural – rather than at the material – level [3]. The use of such parameters tends to attribute ductile characteristics to plain concrete behaviour not compatible with its brittle nature and not justified by the relevant published test data [4-7]. This, in turn, can detrimentally affect the objectivity of the numerical predictions obtained since such parameters often require recalibration depending on the type of problem investigated [3,8,9]. Based on the above, the use of such models is considered generally too complicated for practical applications whilst the results obtained are not always accepted to be reliable and are frequently treated with skepticism. The generality of such models is also limited as they rely on the aforementioned calibration of several parameters for every case considered.

An FE model is generally considered capable of yielding realistic predictions concerning the nonlinear response of concrete structures when the deviation of the predicted values from their experimentally measured counterparts (of particular structural characteristics) does not exceed a value of the order of 20% [3,9,10]. Such structural characteristics usually include the load-bearing capacity, the relation between applied load and corresponding displacements, reactions or first-order deformation derivatives (e.g. rotations). So, in essence, a finite-element analysis (FEA) package is considered to be characterised by both objectivity and generality when it is capable of providing realistic predictions of structural

behaviour for a wide range of structural concrete configurations, without requiring recalibration of the parameters employed by the concrete material model [3,8].

Further to the macro-models, which are widely employed for describing the behavior of concrete and fibre reinforced concrete when assessing structural response, a number of micro-models have been also proposed which aim at providing an in-depth understanding of the effect of fibres on the material behavior of structural concrete [49]. Such models essentially consider the fibres, the various constituents of concrete, as well as their interaction independently, thus offering a more detailed description of the structure of concrete as well as the micro and macro cracking process it undergoes when subjected to external loading [10]. In order to simplify the formulation of such models a homogenization technique is often employed when modelling the concrete medium (due to its heterogeneous nature). However, it should be pointed out, that although micro-level models can be used for studying the behaviour exhibited by small specimens they cannot be easily employed for assessing structural performance. As a result such models are considered beyond the scope of the present work.

The present work is based on the use of a well-known commercial FEA program, ABAQUS [11], capable of carrying out three-dimensional (3D) static and dynamic nonlinear finite element analysis (NLFEA) which incorporates a simple brittle model (termed “brittle cracking model”) in order to describe concrete material behaviour. The latter model is purpose-built for brittle materials the behaviour of which is dominated by tensile cracking [11]. This is largely true in the case of reinforced concrete (RC) flexural structural elements where cracks form due to the development of tensile strains within the concrete medium in the tensile region of the element considered. Such cracks gradually extend (into the compressive region) with increasing levels of applied loading, ultimately leading to structural failure and collapse. This is particularly useful for the present study on the performance of steel fibre reinforced concrete (SFRC) structural configurations as it allows for modelling the effect of steel fibres on the concrete tensile behaviour, especially after the onset of cracking.

It is interesting to note that in the “brittle cracking model”, the behaviour of concrete in compression is modelled essentially as “linear elastic” through the use of an equivalent elastic modulus approximately equal to 50% of secant value of the modulus of elasticity  $E_{\text{cof}}$  concrete for stress levels between 0 and  $0.4f_c$ . The adoption of the latter

assumption/simplification safeguards the numerical stability and robustness of the solution process allowing emphasis to be focused on realistically describing the all-important tensile material behavior of concrete. Although the above assumption may appear at first unreasonable and not representative of concrete material behavior, one should consider that concrete behavior within the compressive region of a flexural member approaching its ultimate limit state is characterised by significant triaxiality [13]. This triaxiality is the result of the penetration of flexural cracking deep into the compressive zone resulting in a certain degree of confinement being imposed onto the ‘uncracked’ concrete of the compressive zone [12,13] (see Fig.1) . Due to this triaxial state of stress the stress-strain curve adopted by concrete design codes to describe concrete material behavior under uniaxial compression which is also used to describe the stress-distribution along the depth of the compressive zone is, at the very best, an approximation which does not describe the true stress distribution in the above region [12,13]. As a result the behavior of concrete in the compressive region of flexural elements differs considerably to that established under uniaxial compression [12] exhibiting a higher load-bearing capacity (approximately 50% higher compared to its counterpart under uniaxial compression) and stiffness. The present investigation reveals that although the model assumes elastic behaviour in compression (mainly for numerical stability purposes), this does not seem to affect accuracy as the predictions obtained concerning certain important aspects of structural response which are in good agreement with their experimentally established counterparts (as discussed in the present study). As a precaution, the compressive strains were also monitored especially when exceeding the ultimate value of 0.0035.

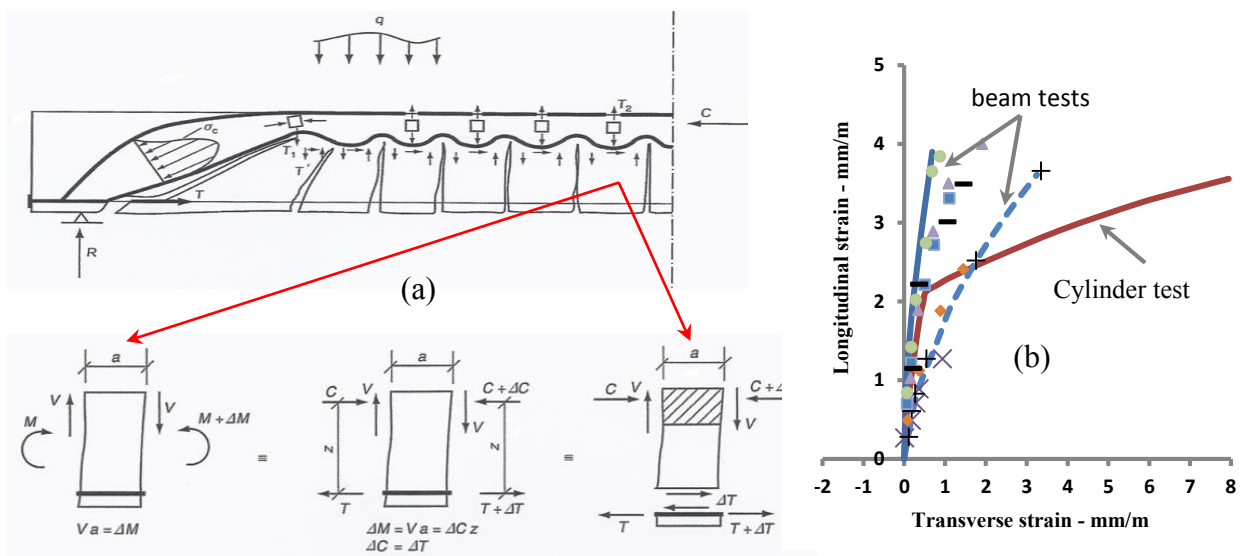


Figure 1: (a) Internal actions developing within RC beams resulting in the development of a triaxial state of stress within the compressive zone [13] and (b) its effect on concrete material behaviour [12].

The “brittle cracking” material model employed (using ABAQUS software) is originally intended for *plain* concrete and was thus modified in order to account for the effect of steel fibres on the cracking processes that concrete undergoes when subjected to tension. The attention of the numerical investigation is focused on: (i) validating the predictions obtained concerning important aspects of the nonlinear behaviour (up to failure) for a wide range of SFRC structural configurations and (ii) investigating their generality and objectivity. The structural configurations considered herein include a wide range of SFRC specimens ranging from simply-supported SFRC beams with no conventional reinforcement to more complex (statically indeterminate, consisting of more than one structural elements and subjected to a combination of axial and lateral loading) SFRC structural configurations fully reinforced. It should be pointed out that although some of the case studies are presented herein for the first time, others have formed the basis for parametric investigations carried out recently assessing the effect of the fibre-content on RC structural responses [14-20]. The reason for presenting all the cases in the present article is to show the objectivity of the numerical model employed. Based on the comparison of the numerical predictions obtained with their experimental counterparts it is shown that, in spite of its simplicity, the model employed herein is capable of providing realistic predictions concerning certain important aspects of structural response (i.e. load-bearing capacity, load-deflection curves, deformation profiles and modes of failure) for all cases of SFRC structural configurations considered without requiring re-calibration.

## 2. MODELLING OF SFRC MATERIAL BEHAVIOUR

To date, a large number of experiments have been conducted in order to determine the effect of steel fibres on structural concrete material behaviour. The vast majority of these tests have been carried out on concrete prisms and cylinders subjected to uniaxial compression, direct or indirect tension and flexure. The aim of these studies is to determine the effect of steel fibres on:

- the compressive  $f_c$  and tensile  $f_t$  strengths, the elasticity modulus  $E_c$ , the stress-strain curve describing the response under uniaxial compression or tension prior and after crack-formation

- the cracking process concrete undergoes when subjected to external loading, which is dependent on a variety of parameters such as the fibre content, the bond strength and 'pull-out' behaviour (exhibited by the fibres bridging a crack as the latter begins to widen and extend with increasing levels of applied load).

The available test data describing SFRC material behaviour is characterised by considerable scatter, which is linked to a number of parameters associated with the steel fibres (i.e. fibre length  $L$ , aspect ratio  $L/d$  with  $L$  being the length and  $d$  the diameter, fibre content  $V_f$ , its shape, strength and orientation) and the concrete mix as well as the mixing process adopted. Based on the available test data, the introduction of steel-fibres into the concrete mix predominantly results in an enhancement of post-cracking behaviour, allowing concrete to exhibit more ductile characteristics compared to the essentially fully brittle behaviour exhibited by plain concrete specimens [4-7, 10]. The fact that this enhancement is mainly observed in tension suggests that the fibres within the concrete mix act primarily in tension, resisting the formation and extension of cracking, whereas in compression one could conservatively assume that their effect could be ignored.

### **2.1. SFRC behaviour in tension**

A number of constitutive models have been proposed to date in the form of stress-strain relationships in order to describe the behaviour of SFRC concrete in tension [21-27]. These models are usually expressed analytically in the form of stress-strain curves consisting of an ascending and a descending branch. Their formulation is either based on the application of regression analysis techniques on data obtained from uniaxial extension or splitting tests [26,27] or on energy approximation methods aiming at assessing the variation of the level of energy absorbed (toughness) during flexure testing of SFRC prisms [21-24].

In spite of the above different approaches employed, all the models clearly indicate that the portion of the stress-strain relationship mainly affected by the introduction of steel fibres in the concrete mix is associated with the post-cracking behaviour of SFRC. This allows the latter material to exhibit more ductile characteristics compared to the fully brittle behaviour exhibited by plain concrete [10]. Depending on the amount and type of fibres used, the post-cracking behaviour is described either by a strain-softening or hardening branch of the stress-strain curve. The residual strength exhibited after cracking is the result of the combined action of the steel-fibres bridging the cracks and the bond developing between

the fibres and the surrounding concrete. The use of moderate fibre contents normally results in a softening post-crack behaviour exhibiting ductile characteristic (or a strain-hardening response in the case of high fibre contents) as the fibres are able to undertake the tensile forces which act in a direction normal to the plane of the crack (thus potentially leading to an increase in residual tensile strength). This type of behaviour is associated with the formation of multiple cracks [28,29] with the fibres ultimately exhibiting pull-out failure [25,27,30]. The latter depends largely on the bond strength between fibres and surrounding concrete.

Two constitutive models are presently employed [26,27] to describe the post-cracking SFRC behaviour, which is dependent on the fibre content as well as the shape and size of the fibres. The main reason for selecting these models is due to the simplicity which characterises their analytical formulation and their generality as they allow for any aspect ratio to be modelled as well as the bond between the concrete and fibres (several other models were also considered initially as discussed elsewhere [14]). The analytical formulations of both models are presented below in the form of stress-strain relationship:

$$\begin{aligned}
 \sigma &= f_t [2(\varepsilon/\varepsilon_{t0}) - (\varepsilon/\varepsilon_{t0})^2] && \text{for } (0 \leq \varepsilon \leq \varepsilon_{t0}) \\
 \sigma &= f_t [1 - (1 - f_{tu}/f_t)(\varepsilon - \varepsilon_{t0}/\varepsilon_{t1} - \varepsilon_{t0})] && \text{for } (\varepsilon_{t0} \leq \varepsilon \leq \varepsilon_{t1}) \\
 \sigma &= f_{tu} && \text{for } (\varepsilon_{t1} \leq \varepsilon \leq \varepsilon_{tu}) \\
 \sigma &= f_{tu} - f_{tu}(\varepsilon - \varepsilon_{t1})/(\varepsilon_{tu} - \varepsilon_{t1}) && \text{for } (\varepsilon_{t1} \leq \varepsilon \leq \varepsilon_{tu})
 \end{aligned} \tag{1}$$

[26]      [27]

where  $f_t$  and  $\varepsilon_{t0}$  are the ultimate tensile strength and strain (i.e. at onset of cracking), respectively, whereas  $f_{tu}$  and  $\varepsilon_{t1}$  are the residual strength and corresponding strain of SFRC defined as:

$$f_{tu} = \eta \cdot V_f \cdot \tau_d \cdot L/d \quad \text{and} \quad \varepsilon_{t1} = (\tau_d \cdot L)/(d \cdot E_s) \tag{2}$$

where

$\eta$  is the fibre orientation factor, takes values between 0.405 to 0.5 and accounts for the random distribution of fibres.

$V_f$  is the fibre content expressed as the volume fraction

$\tau_d$  is the bond stress developing between the steel fibres and the surrounding concrete in which it is anchored

$L/d$  is the aspect ratio of the steel fibre (with  $L$  being the length and  $d$  the diameter)

$E_s$  is the modulus of elasticity of steel fibres.

## 2.2. SFRC behaviour under uniaxial compression

In the case of uniaxial compression, available test data shows that the compressive strength and the maximum compressive strain attained prior to failure increase with increasing levels of fibre-content [21,24,25,30-32]. This is owed to the confinement effect that the fibres impose on the concrete specimens (mainly cylinders) when tested under uniaxial compression allowing concrete to exhibit behaviour with more ductile characteristics [33-37]. However, these effects are not easily quantified due to the scatter characterising the relevant published test data. As a result it is usually conservatively assumed that the stress-strain curve describing the SFRC behaviour in uniaxial compression is not significantly affected by the use of steel fibres and as a result it can be considered the same as that corresponding to plain concrete.

## 2.3. Modelling of cracking

As stated earlier, the “brittle cracking model” in ABAQUS [11] was adopted for modelling concrete in the present work as the material behaviour is dominated by tensile cracking. In the model, the cracking process that concrete undergoes is modelled using the smeared crack approach [10,38,39], in the sense that it does not track individual “macro” cracks. Constitutive calculations are performed at each integration point of the finite element model and the presence of cracks enters into these calculations by adjusting the stress and material stiffness associated with the integration point [11]. A crack is considered to form when the predicted stress in a given part of the structure corresponds to a point in the principal stress space that lies outside the surface defining the failure criterion for concrete, thus resulting in localised failure of the material. The plane of the crack is assumed normal to the direction in which the smallest principal stress acts (smallest compressive or largest tensile stress). A simple Rankine failure criterion is used to detect crack initiation (i.e. a crack forms when the maximum principal tensile stress exceeds the specified tensile strength of concrete). Constitutive calculations are performed independently at each integration point of the finite element model. The presence of cracks enters into these calculations by the way in which the cracks affect the stress and material stiffness associated with the integration point. After

crack formation the residual shear stiffness along the plane of the crack is determined through the use of a “shear retention” factor. Its value is affected by the presence of the fibres bridging the two sides of the crack. The shear stiffness is considered to decrease as cracks widen. Therefore, in order to allow for degradation in shear stiffness due to crack propagation, the shear modulus is reduced linearly from full shear retention (i.e. no degradation) at the cracking strain to 50% of that at the ultimate tensile strain. It is worth noting that the shear retention does not diminish altogether due to the presence of the fibres which enhance dowel action as well as aggregate interlock by reducing crack opening. Crucially, the fibres contribute to shear resistance by providing tensile resistance (across the crack) to the shear induced “diagonal tension” stresses.

### **3. Nonlinear strategy adopted**

The present numerical investigation employs an explicit dynamic solver available in ABAQUS [11] to carry out quasi-static analysis by imposing the external action with a low rate of loading in order to render the effect of inertia insignificant. This was intended to ensure the efficiency and stability of the numerical solution. Therefore in the present study, the “brittle cracking model” was used in conjunction with ABAQUS/Explicit [11]. The explicit, dynamic procedure allows for executing a large number of small time increments efficiently. In this method, small fairly inexpensive increments are used as an explicit central-difference time integration rule is utilised, where there is no solution for set of simultaneous equations (as is the case with the implicit method). An iterative procedure based on the well-established Newton-Raphson method is employed in order to effectively account for the stress redistributions during which the crack formation and closure checks as well as convergence checks are carried out. 3D modelling was adopted throughout the present study in order to detect the principal tensile stress in a true tri-axial state of stress. Thus, the concrete medium is modelled by using a dense mesh of 8-node brick elements. The element formulation adopts a reduced integration scheme to avoid numerical instabilities due to locking. The concrete model adopts fixed, orthogonal cracks, with the maximum number of cracks at a material point limited by the number of direct stress components present at that material Gauss point of the finite element model (i.e. a maximum of three cracks in the three-dimensional modelling adopted in the present study). The ratio between kinetic and strain energies is checked to ensure that it remains below ~5% indicating that the analysis remains quasi-static. In addition to the numerically-based divergence failure criterion,

Careful consideration was also given to the kinetic energy levels developed during the FE runs and a sudden large jump was taken to denote failure. This is because such sudden spikes are likely to be due to excessive cracking and deformation impairing the structural integrity. A similar approach is commonly used in the modelling of RC structures (e.g. Zheng et al. [40]). This was also confirmed by examining both the deformed shape and cracking pattern of the structure, as well as ensuring that the compressive strains does not significantly exceed the critical value of 0.0035 before failure. In the present numerical studies, the load was applied using a displacement-based method to minimise convergence problems.

#### **4. FE modelling of structural forms investigated**

A mesh sensitivity analysis was carried out in order to select the best mesh size to be used and to avoid mesh dependency. Thus, the calibration work carried out against experimental data was crucial in selecting the best mesh size that will accurately represent the true structural response. Detailed calibrations were carried out as part of the present investigations at both the material and structural levels (e.g. notched SFRC beams for the former, simply-supported beams and statically-indeterminate columns), which are discussed in the present paper. The concrete medium is modelled by using a dense mesh of 3D brick elements with an edge size between 10 and 30 mm. It should be noted that the size of the finite elements used is determined based on the size of the specimen used to derive the stress-strain curves adopted for describing the behaviour of SFRC in tension (described by Eq.1).

Reinforcement bars are modelled by 2-node single Gauss point truss elements with sectional areas distributed to the relevant nodes of the beams' cross-section so as to be equivalent, in terms of both cross-sectional area and location, to the actual reinforcement of the beam specimen. Truss elements representing the steel reinforcement are placed along successive series of nodal points in both vertical and horizontal directions, in order to simulate both longitudinal bars and transverse stirrups. Since the spacing of these line elements was predefined by the location of the brick elements' nodes, their cross-sectional area was adjusted so that the total amount of both longitudinal and transverse reinforcement to be equal to the design values. Because of the double symmetry of the problem at hand, one quarter of the actual specimen was modelled with suitable symmetry boundary conditions. The external load was applied to the FE model (representing the structural configuration) in

the form of displacement increments through rigid elements similar in shape and size to the steel platens used in the experiment. Rigid elements were used to form a vertical support on the bottom face close to the edge of the beam. The rigid elements were employed in order to effectively distribute the applied point loads or reaction forces and avoid the development of high stress concentrations that can result in premature localised cracking/failure (at the supports or at the point where the external load is applied) and numerical instabilities.

## 5. Conventional RC simply-supported beams

Initially the behaviours of two simply-supported RC beams are investigated under monotonic static loading applied at their mid-spans. The responses of these beams have been established experimentally in the past [41,42]. The first of the two beams presently considered [41] exhibits ductile behaviour (i.e. flexural failure mode), whereas the second beam [42] fails in a brittle manner (i.e. shear failure mode). The design details of the ductile beam are presented in Fig.(2a). The modulus of elasticity ( $E_s$ ), yield stress ( $f_y$ ), and ultimate strength ( $f_u$ ) of both the longitudinal and transverse reinforcement bars used are 206 GPa, 460 MPa and 560 MPa, respectively, with the compressive strength ( $f_c$ ) of concrete being 45 MPa. Failure of the specimen was caused by yielding of the longitudinal reinforcement bars in the mid-span region of the specimen, resulting in the formation of extensive flexural cracking which penetrate deep into the compressive region of the RC beam leading ultimately to failure of concrete in that region. The design details of the brittle beam [42] are presented Fig.(2b). The values of  $E_s$ ,  $f_y$  and  $f_u$  of the reinforcement bars used are 200 GPa, 555 MPa and 958 MPa, respectively, whilst the value of  $f_c$  of the concrete used was 22.5 MPa. Failure was abrupt and occurred after the formation of inclined cracks along the shear span. The FE models representing the beams specimens currently considered are presented in Fig.3. In both cases good correlation is observed between the experimentally and numerically established response expressed in the form of load- (mid-span) deflection curves presented in Fig.3 as the numerical model employed, despite its simplicity, is able to accurately predict both ductile and brittle response types exhibited by the beam specimens presently considered.

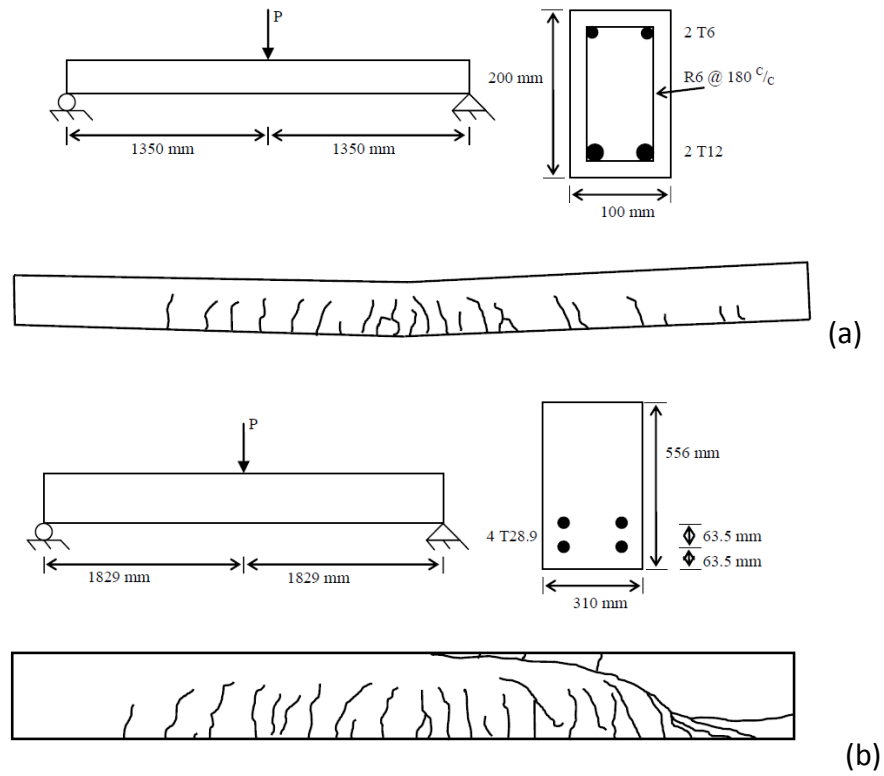


**Fig. 2:** Reinforcement and loading details and cracking patterns for RC simply-supported beams exhibiting (a) ductile [41] and (b) brittle [42] modes of failure

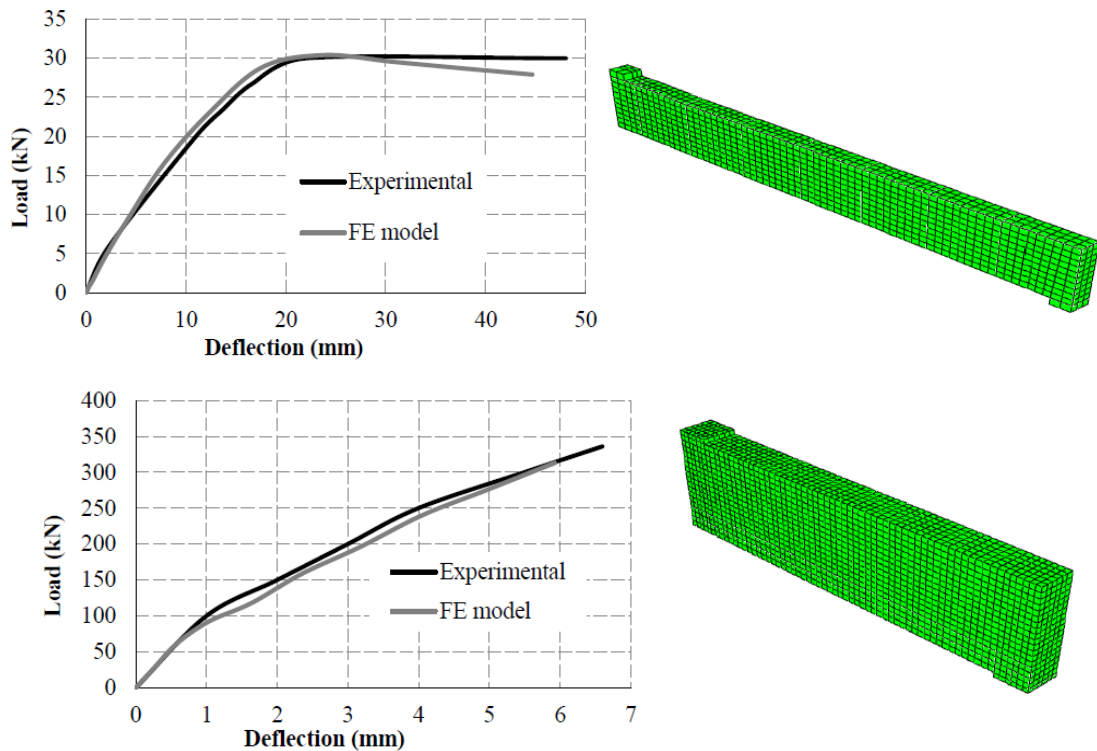


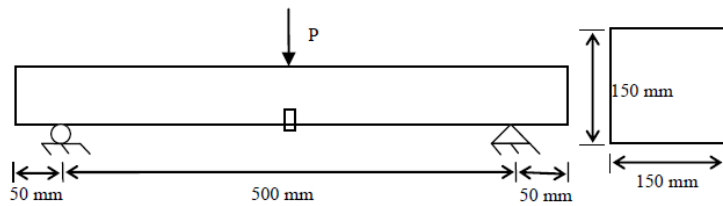
**Fig. 3:** FE mesh and comparison between experimental and numerical results for RC simply-supported beams exhibiting (a) ductile [41] and (b) brittle [42] modes of failure

## 6. Simply-supported SFRC beams with no conventional reinforcement

In order to assess the contribution of steel fibres to the behaviour of structural concrete at both *material* and *structural* levels, a number of experimental studies were carried out investigating the responses of simply-supported SFRC beam specimens with and without conventional reinforcement. The first set of experiments focused on short (i.e. span not longer than 500 mm) notched beams which were reinforced solely by fibres and thus represent the response at the material level. The second set was focused on larger beams with both fibre and conventional bar reinforcement and therefore capture the response at the structural level. Both sets of experiments were modelled in the present FE studies and the results of the first are discussed in this section, whilst the findings of the second are discussed in the subsequent section. It must be pointed out that the notched beam samples – of spans not exceeding 500 mm – are in line with standard testing methods for SFRC such as those recommended by RILEM [29], which are aimed at establishing the tensile characteristics at the material level (albeit indirectly using a flexural test rather than a direct tensile test due to the practical difficulty of performing the latter). This is the reason why such specimens were described as being at the material level, although it can be argued that they resemble a structure as well. This caveat is important to avoid confusion regarding the meaning of the word “material” in the context of the current study.

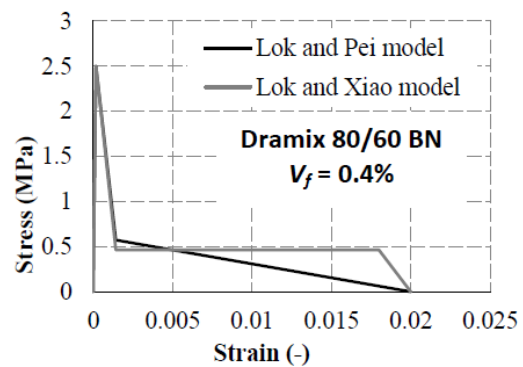
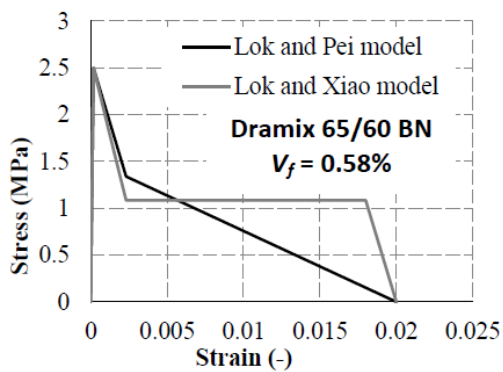
In the first study, the experiments considered were those carried out on beams without conventional reinforcement subjected to 3-point [23,43] and 4-point [25,44] bending tests. These were small beam specimens which, as explained above, allow further insight into how the fibres interact with structural concrete resulting in a shift in specimen behaviour at the *material* level. Therefore, the ensuing FE-based case studies were aimed at stimulating these experiments in order to evaluate the accuracy of the two constitutive models presented earlier [26,27]. At the same time, the modelling of the experiments in the present section was also useful in assessing the ability of the material models and FEA strategy to realistically predict the response of simply-supported SFRC beams with no conventional reinforcement. The design details of the SFRC notched beam specimens subjected to 3-point bending tests [23,43] accompanied by the stress-strain curves adopted for describing the tensile behaviour of SFRC [26,27] for each specimen are presented in Figs 4 and 5. Similarly, the design details of the SFRC beams subjected to 4-point bending tests [25,44] together with their corresponding tensile stress-strain curves are presented in Figs 6 and 7. A summary of the

key values of fibres and concrete properties are summarised in a tabular form underneath the figures as well. A dense FE mesh consisting of 8-node brick FE elements with a width of 25mm was adopted to model the beam specimens. The comparisons between the numerical predictions and their experimental counterparts presented in Figs 8 to 11 (in the form of load-deflection curves) reveal good agreement both before and after the load-bearing capacity was attained.



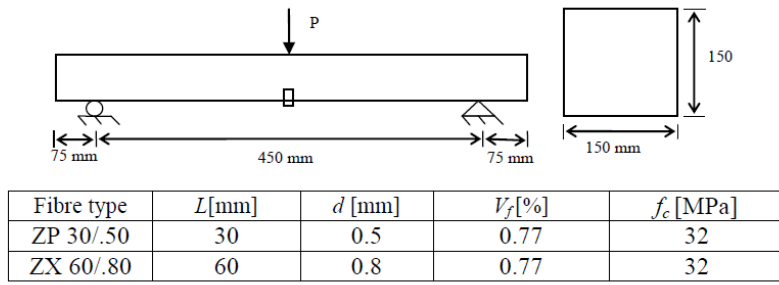
Fibre type	$L$ [mm]	$d$ [mm]	$V_f$ [%]	$f_c$ [MPa]
Hooked end	60	0.90	0.58	25
Hooked end	60	0.75	0.40	25

(a)

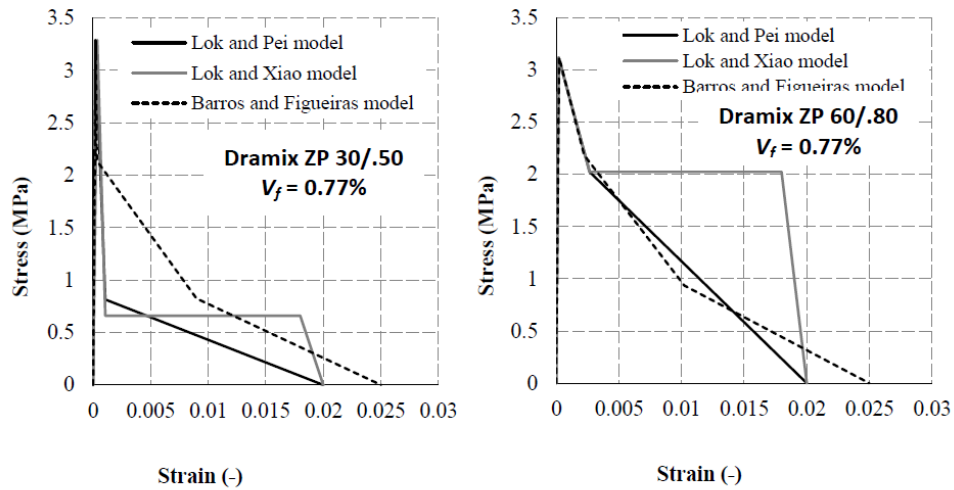


(b)

**Fig. 4:** Modelling of notched SFRC beam tests by Barros *et al.* [43]: (a) design details and material properties and (b) stress-strain curves describing SFRC tensile behaviour

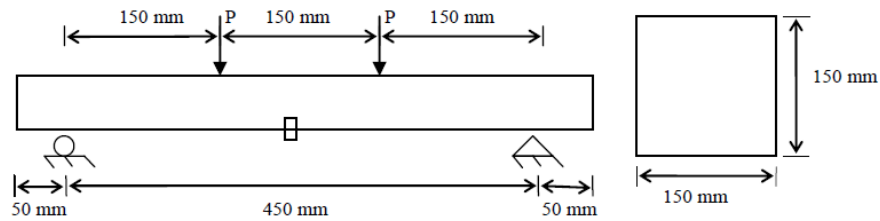


(a)



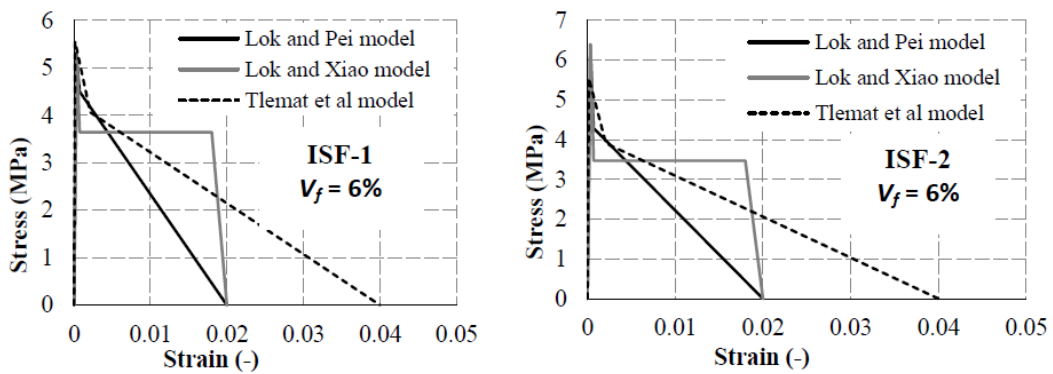
(b)

**Fig. 5:** Modelling of notched SFRC beam tests by Barros and Figueiras [23]: (a) design details and material properties and (b) tensile stress-strain curves for SFRC



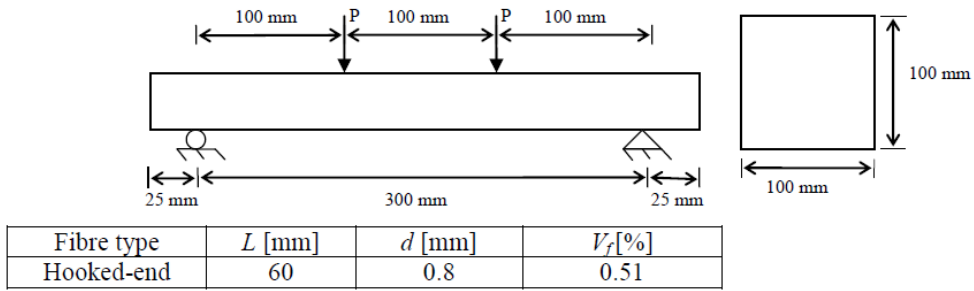
Fibre type	$L$ [mm]	$d$ [mm]	$V_f$ [%]
ISF-1	50	1.00	6.0
ISF-2	50	1.05	6.0

(a)

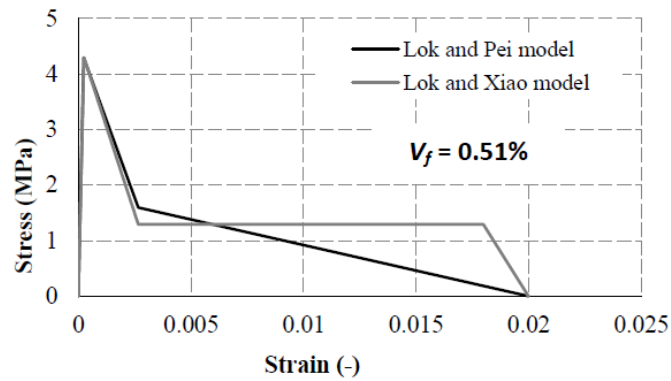


(b)

**Fig. 6:** Modelling of notched SFRC beam tests by Tlemat *et al.* [25]: (a) design details and material properties and (b) tensile stress-strain curves for SFRC



(a)



(b)

**Fig. 7:** Modelling of SFRC beam tests by Trottier and Banthia [44]: (a) design details and material properties and (b) tensile stress-strain curves for SFRC

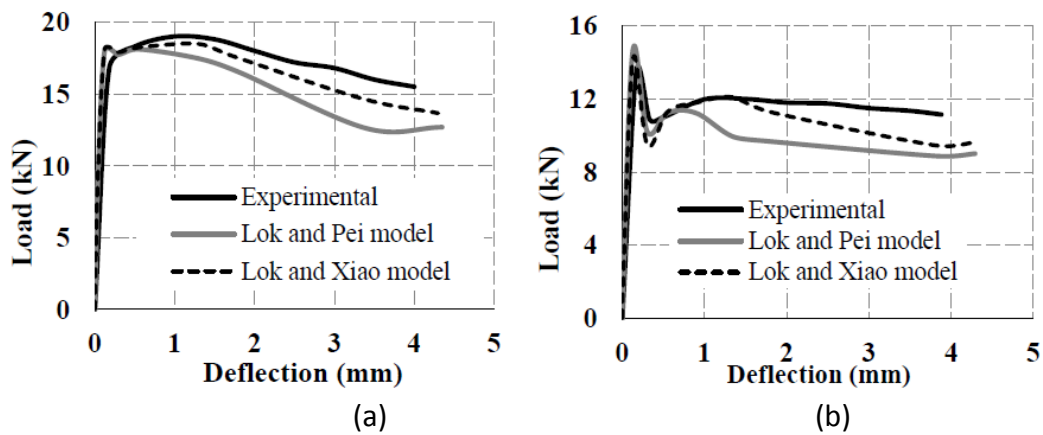


**Fig. 8:** Comparison between experimental and numerical results for Barros et al. [43] notched SFRC beams using (a) Dramix 65/60 BN fibres with  $V_f = 0.58\%$  and (b) Dramix 80/60 BN fibres with  $V_f = 0.4\%$ .

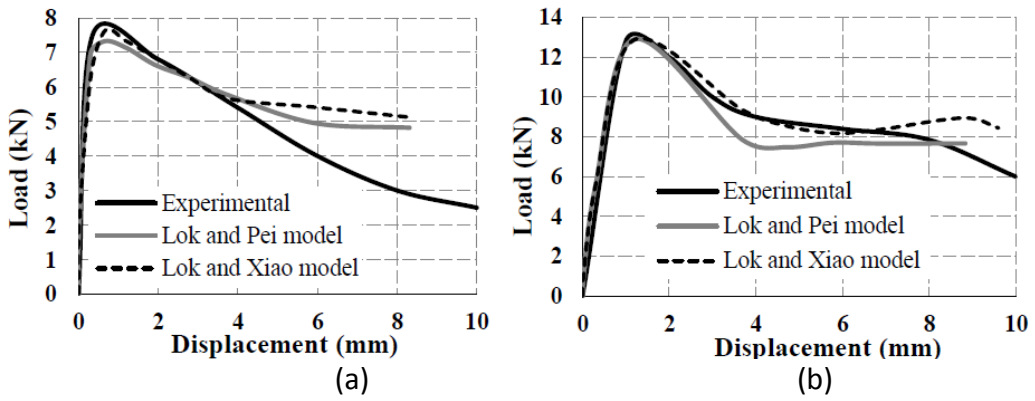


**Fig. 9:** Comparison between experimental and numerical results for Barros and Figueiras [23] notched SFRC beams with  $V_f = 0.77\%$  using (a) Dramix ZP 30/.50 and (b) Dramix ZP 60/.80 fibres

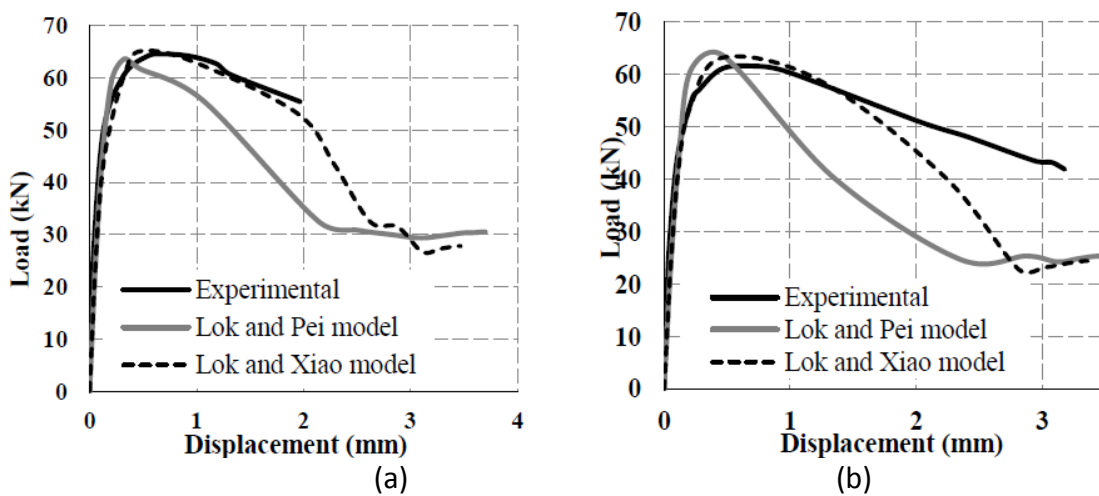


**Fig. 10:** Comparison between experimental and numerical results for Tlemat et al. [25] notched SFRC beams with  $V_f = 6\%$  using (a) ISF-1 and (b) ISF-2 fibres

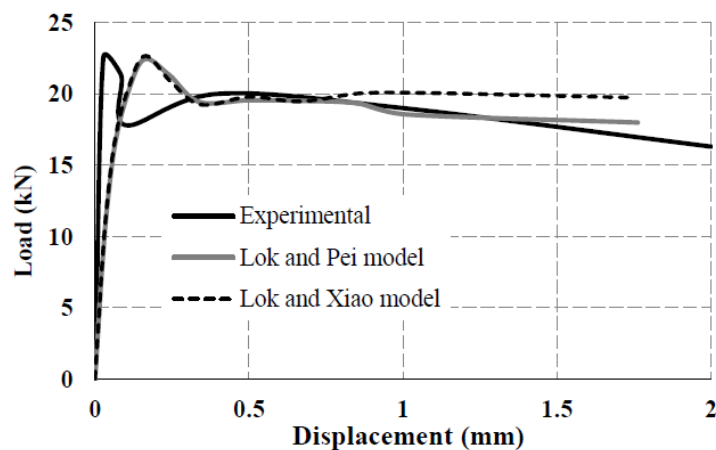
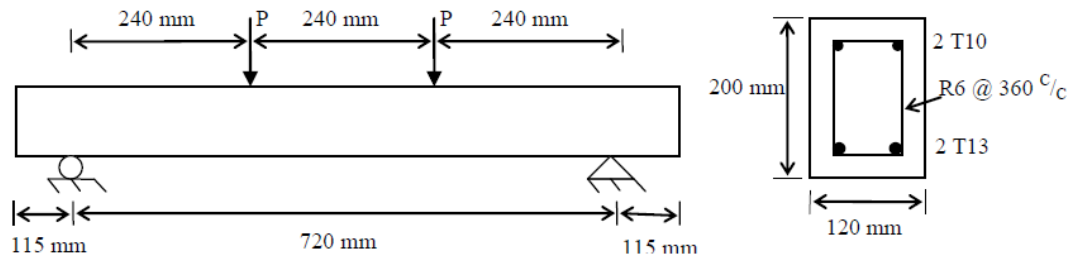


**Fig. 11:** Comparison between experimental and numerical results for Trottier and Banthia [44] SFRC beams with  $V_f = 0.51\%$ .

## **7. Simply-supported SFRC beams with conventional reinforcement under monotonic loading**

In the present section, the predictions of the proposed FEA model are validated against experimental results for simply-supported SFRC beams containing both fibres and conventional (i.e. longitudinal and transverse) steel reinforcement, unlike the specimens in the previous section which had no conventional reinforcement. The beams are also larger than the ones considered in the previous section and thus allow an examination of the responses at the *structural* level, as explained earlier. The dimensions, reinforcement and loading details of the simply-supported beam specimens tested by Cho and Kim [30], Oh *et al.* [35] and Sharma [33] are depicted in Figs 12 to 14 accompanied by the stress-strain curves adopted in the corresponding FE study for describing the tensile behaviour of SFRC. As in the preceding case studies considered, a dense FE mesh consisting of 8-node brick FE elements with a width of 25 mm was adopted to model the beam specimens. Elastic steel plates were added at the support and loading regions to mimic the experimental setup and help avoid the development of high stress concentrations which can potentially lead to numerical instability and premature localised failure. The comparison between the numerical and experimental results presented in Figs 15 to 17 show that there is good agreement between the two sets of data. The responses of the SFRC beam specimens tested by Cho and Kim [30] and Oh *et al.* [35] exhibited a ductile failure mode. On the other hand, the beam tested by Sharma [33] were intended to examine the shear behaviour and thus has failed in a brittle manner. From the comparisons, it can be seen that the FE model presently employed was capable of providing accurate predictions for both modes of structural failure. As part of the current research project, further studies were carried out on the shear responses of SFRC simply-supported as discussed elsewhere [17]. Considering the findings in the preceding two sections, it can also be concluded that the FE model was successful in predicting the behaviour at both material and structural levels. To expand the study further, different structural configurations other than simple supports were considered (such as statically-indeterminate elements and column-beam joints), which will be discussed in subsequent sections.



Fibre type	$L$ [mm]	$d$ [mm]	$V_f$ [%]	$f_c$ [MPa]
Hooked-end	36	0.6	1.0	25.3
Hooked-end	36	0.6	1.5	23.9
Hooked-end	36	0.6	2.0	28.8

Material properties of SFRC

$E_s$	$f_y$	$f_u$
200 GPa	400 MPa	600 MPa

Material properties of steel reinforcement

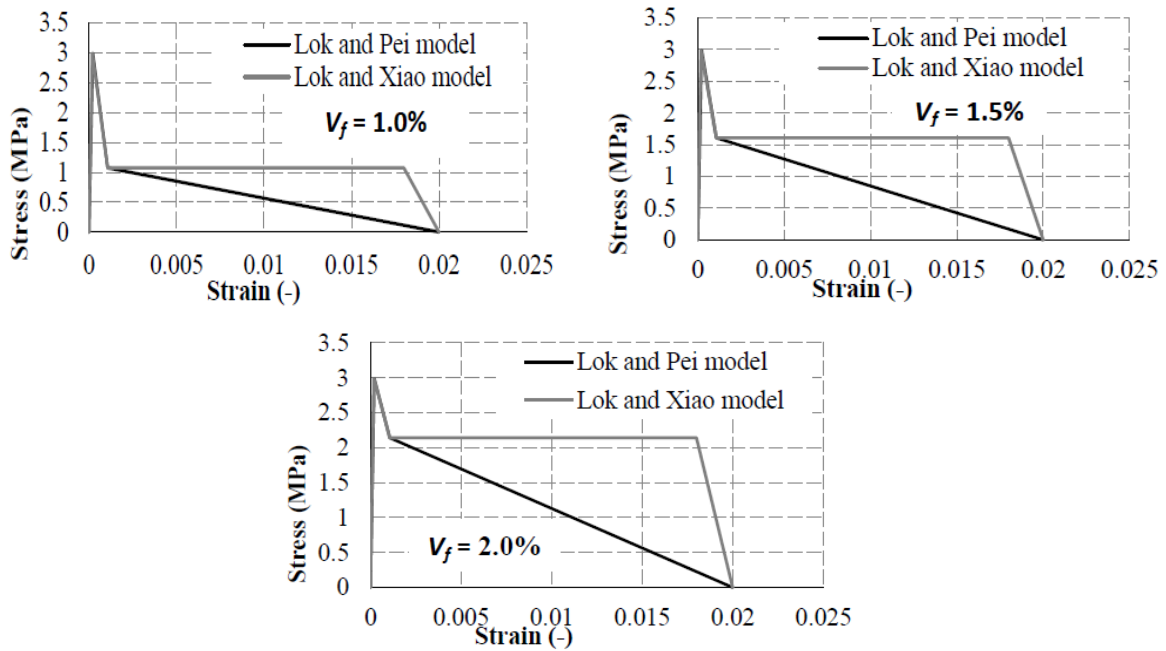
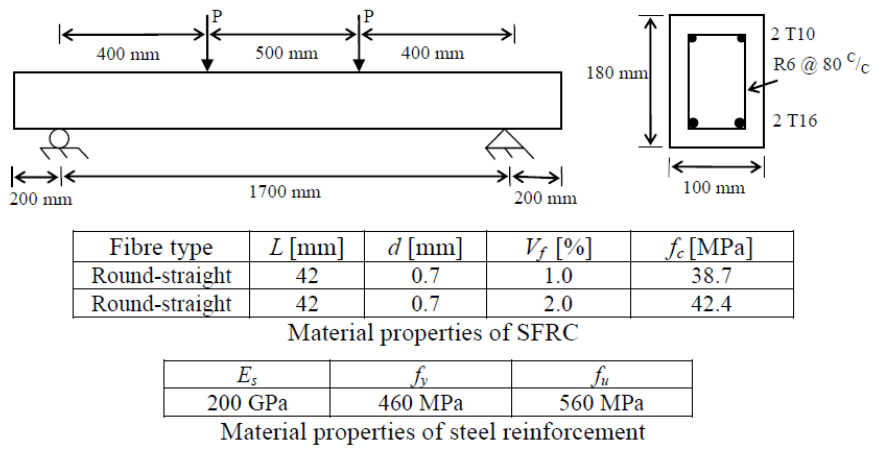


**Fig. 12:** Modelling of simply-supported beams tested by Cho and Kim [31]: (a) design details and material properties and (b) tensile stress-strain curves for SFRC



(a)

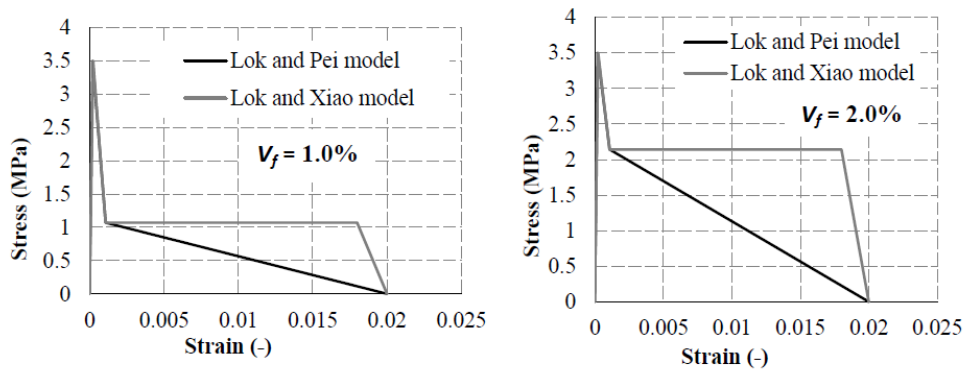
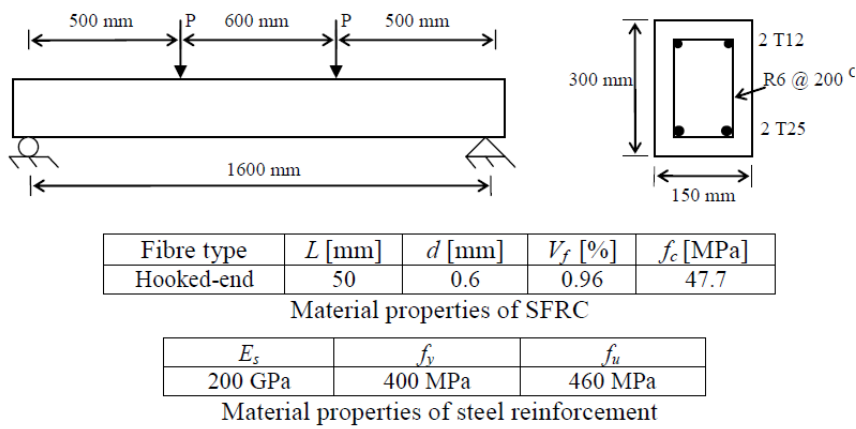


**Fig. 13:** Modelling of simply-supported beams tested by Oh *et al.* [35]: (a) design details and material properties and (b) tensile stress-strain curves for SFRC



(a)

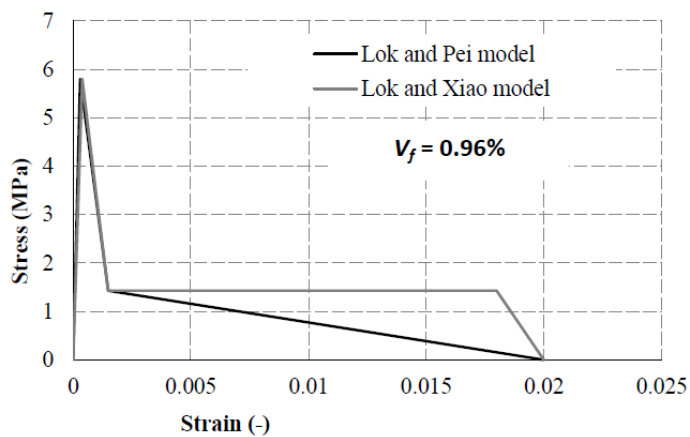


**Fig. 14:** Modelling of SFRC simply-supported beams tested by Sharma [33]: (a) design details and material properties and (b) tensile stress-strain curves for SFRC

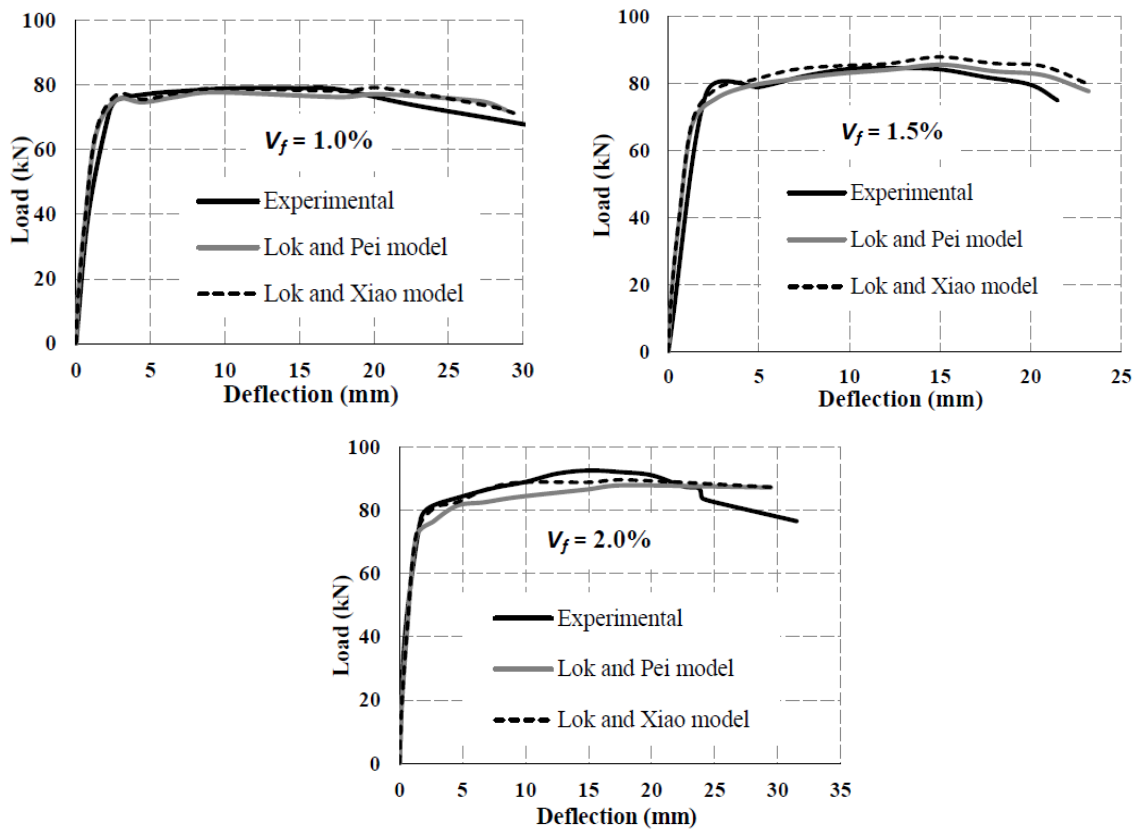


**Fig. 15:** Comparison between experimental and numerical results for Cho and Kim [30] simply-supported beams with  $V_f =$  (a) 1.0%, (b), 1.5% and (c) 2.0%

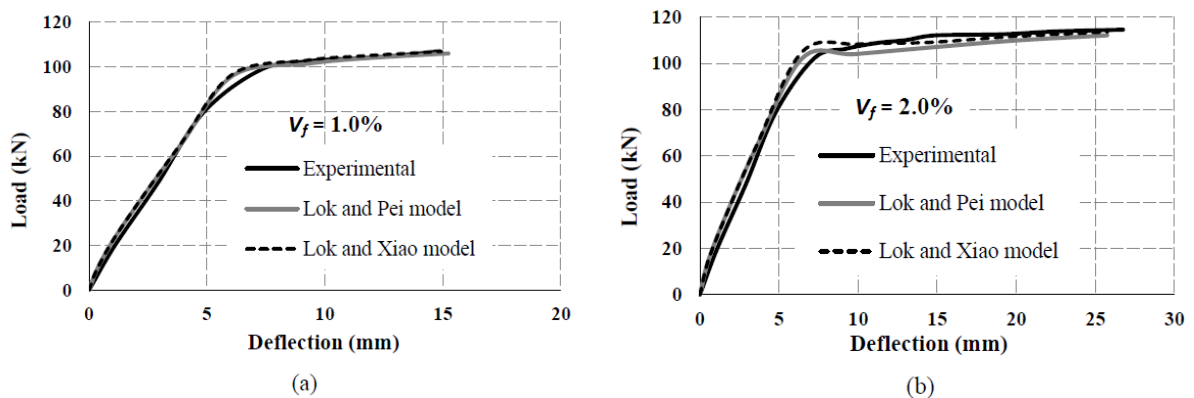


**Fig. 16:** Comparison between experimental and numerical results for Oh et al. [35] simply-supported beams with  $V_f =$  (a) 1.0% and (b) 2.0%

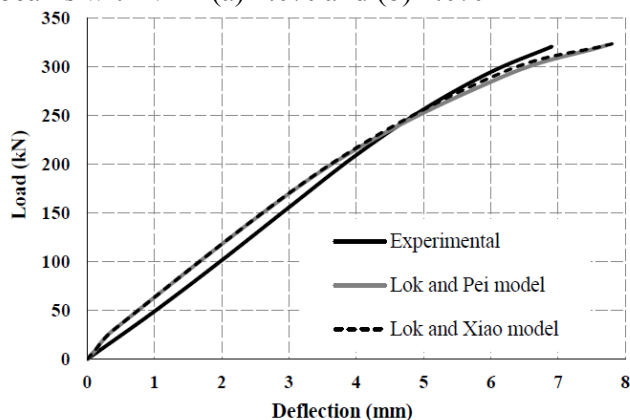
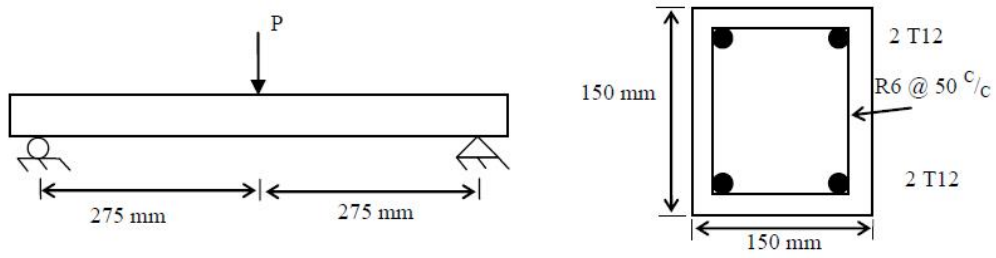


**Fig. 17:** Comparison between experimental and numerical results for the case of simply-supported beams Sharma [33] with  $V_f = 0.96\%$

## **8. Simply-supported SFRC beams with conventional reinforcement under cyclic loading**

Imposing a cyclic load on a SFRC structural form causes the formation and closure of a number of cracks during each load reversal. The cracking procedure that the structure undergoes during each load cycle leads to a gradual degradation of the concrete medium which may ultimately affect its load-carrying capacity. Therefore, the case of cyclic loading offers a strenuous test of the validity of the proposed FE model and associated numerical strategy and its ability to accurately model the crack opening and closure procedure that the concrete medium undergoes during the application of each load cycle and the role of fibres. Such a test is considered to be essential before attempting to extend the use of the model for the analysis of RC structures under seismic action.

In order to assess the ability of the FE model presently adopted to predict the structural responses under cyclic loading, the behaviour of simply-supported SFRC beams was investigated under lateral loads applied both monotonically up to failure as well as in the form of load cycles. The behaviour of the specimen at hand was established experimentally under both types of loads by Campione and Mangiavillano [31]. The salient features of the beam, numerical and material arrangements adopted are shown in Fig. 18. Taking advantage of the symmetrical conditions at the mid-span and along the beam, only one-quarter of the beam was modelled as depicted in Fig. 18(b). The experimental and corresponding FE-based results obtained describing the responses of the beam are presented in Fig. 19 in the form of load-deflection curves. The failure criterion for the numerical predictions of load-deflection curves is also shown, which was defined based on an examination of the kinetic energy levels (depicted in Fig. 19) and a sudden jump was taken to denote failure. This is because a high kinetic energy is likely to be the result of excessive movement of the structure indicating extensive cracking and deformation associated with structural failure (i.e. impairment to structural integrity). This is a common approach used in the numerical modelling of RC structures (e.g. Zheng *et al.* [40]). This was also confirmed by examining both the deformed shape and cracking pattern of the structure. The comparison of the numerical predictions with their experimental counterparts shows reasonable agreement between the two sets of data. The numerical results for the cyclic load case show a failure point slightly earlier than the one found experimentally. However, the difference is small and the FE results are on the safe side (it could also be argued that the additional small part in the experimental data has started after the onset of failure and thus should be discounted).



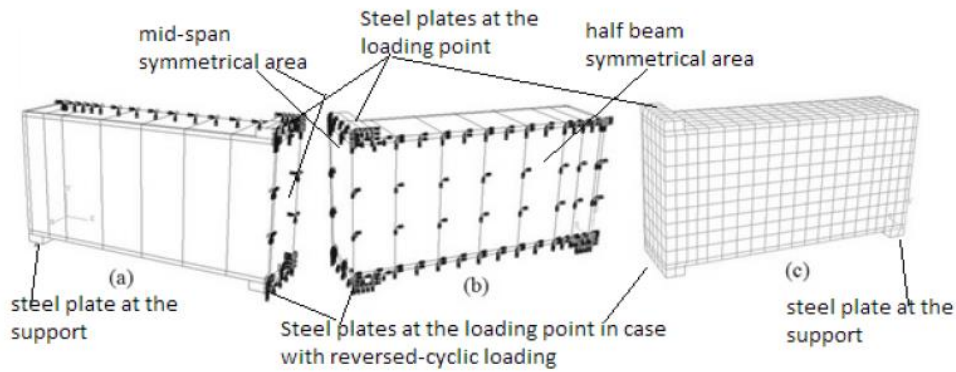
Fibre type	$L$ [mm]	$d$ [mm]	$V_f$ [%]	$f_c$ [MPa]
Hooked-end	30	0.5	1.0	25.3
Hooked-end	36	0.6	1.5	23.9

Material properties of SFRC

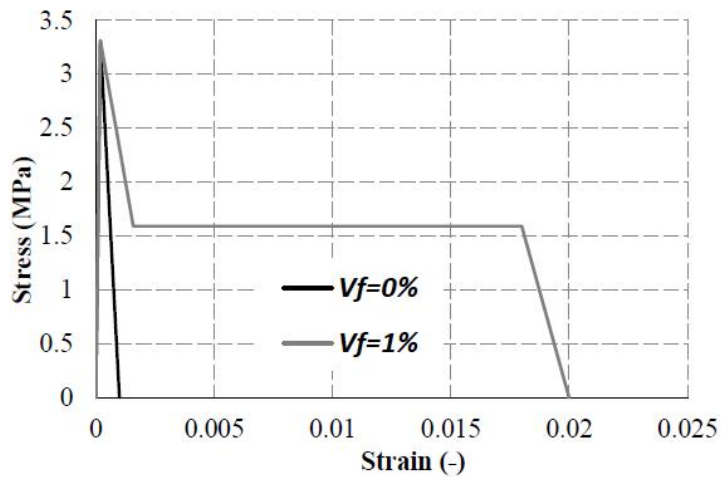
$E_s$	$f_y$	$f_u$
200 GPa	400 MPa	600 MPa

Material properties of steel reinforcement

(a)



(b)



(c)

**Fig. 18:** Modelling of beam tests by Campione and Mangiavillano [31]: (a) design details and material properties, (b) FE mesh and symmetrical arrangement used and (c) tensile stress-strain curves for SFRC and plain concrete (i.e.  $V_f = 0\%$ )

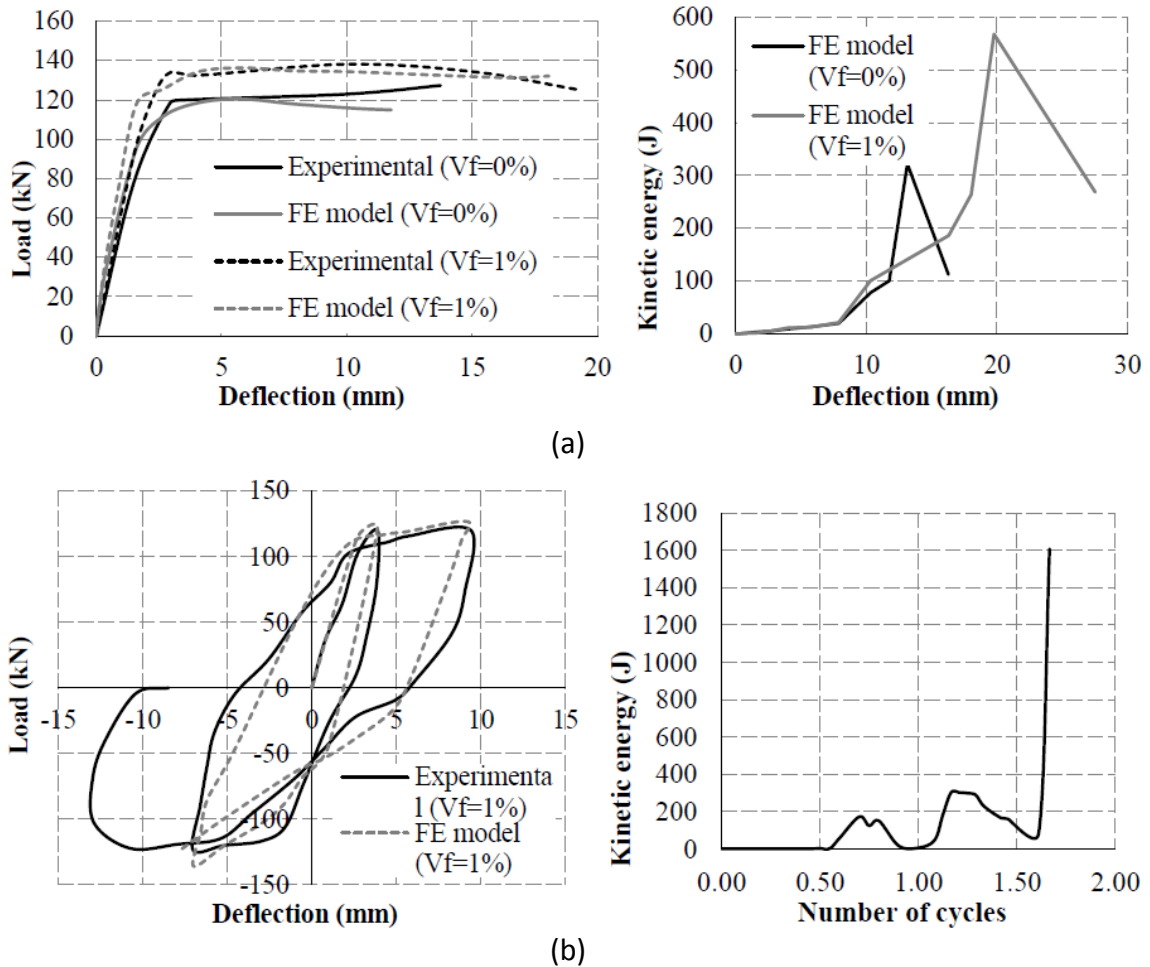
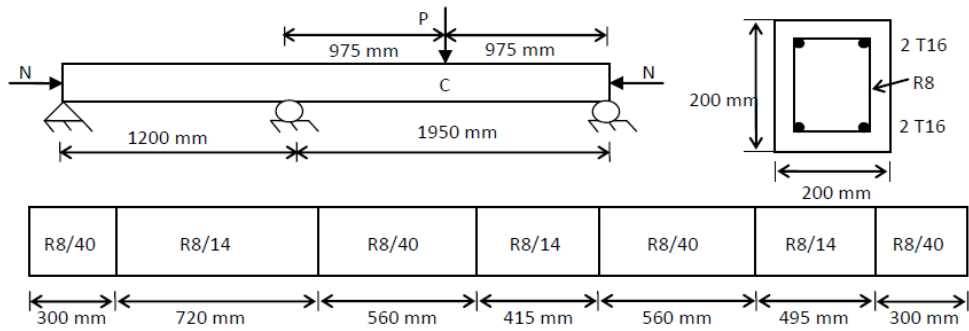


**Fig. 19:** Comparison between experimental and numerical results for simply-supported beams Campione and Mangiavillano [31] under (a) monotonic loading and (b) cyclic loading, and corresponding kinetic energy profiles used to determine failure

## 9. Statically-indeterminate SFRC columns subjected to combined axial and lateral loading

Most of the studies on SFRC structural elements available in the literature are concerned with simply-supported configurations, which have been examined in the preceding sections. In the present study, consideration was also given to statically-indeterminate arrangements in order to ascertain the ability of the adopted FE model in accurately predicting the responses of these forms. To achieve this, two-span SFRC continuous columns under a constant axial load combined with a lateral load (applied either monotonically or in reversed cycles) were studied. The specimens adopted for the present validation purposes were those tested by Kotsovos *et al.*[45] and were referred to as D16-FC30-M and D16-FC30-C in the experimental work under monotonic and cyclic loading, respectively. Their main characteristics are summarised in Fig. 20, which also shows the material properties and loading histories adopted for FE modelling.

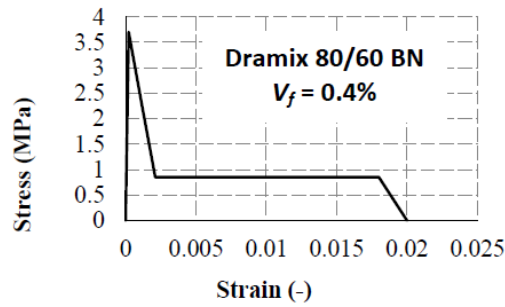


Fibre type	$L$ [mm]	$d$ [mm]	$V_f$ [%]	$f_c$ [MPa]
Hooked-end	60	0.75	0.4	37

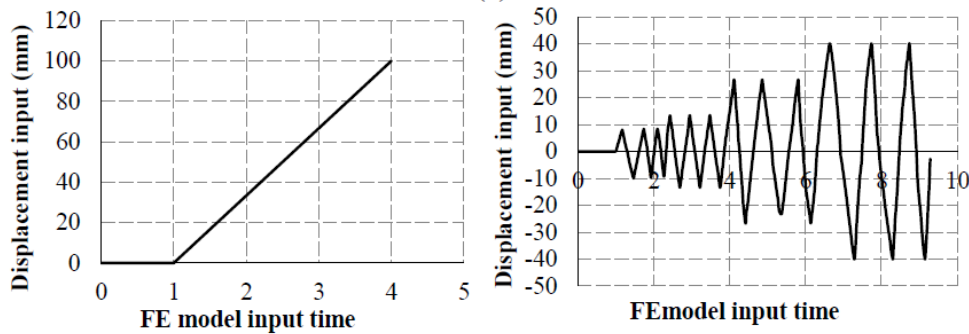
$E_s$ [GPa]	$f_y$	$f_u$
200	556	743

Material properties of steel reinforcement

(a)



(b)



(c)

**Fig. 20:** Statically-indeterminate columns tests by Kotsovos *et al.* [45]: (a) design details and material properties, (b) stress-strain curves describing SFRC tensile behaviour and (c) monotonic and cyclic loading histories

The experiments were aimed to mimic the response of a column under both gravity and lateral monotonic or seismic (i.e. cyclic) loads, which are represented by an axial force (N) and a lateral load (P) in Fig. 20(a). The statically-indeterminate arrangement also allows for a study of the effect of fibres on strength, ductility as well as moment redistribution and formation of plastic hinges. The discussion presented herein is limited to the validation of the FE model against the experimental data, whilst the findings from an FE-based full

parametric study carried out on these columns under both types of lateral loading can be found elsewhere [18,19]. For FE modelling purposes, the lateral load (whether monotonic or cyclic) was applied using a displacement-based method at point C in Fig. 19(a) and the corresponding time histories adopted are depicted in Fig. 20(c). The resulting load-deflection curves together with their experimental counterparts are shown in Fig. 21 (the failure criterion – discussed earlier – identified by a sudden jump in kinetic energy indicating excessive cracking is also presented). The good agreement between experimental and numerical results for the SFRC columns (for both monotonic and cyclic load cases) confirms the validity of the FE model to simulate the behaviour of such statically-indeterminate SFRC structural elements.

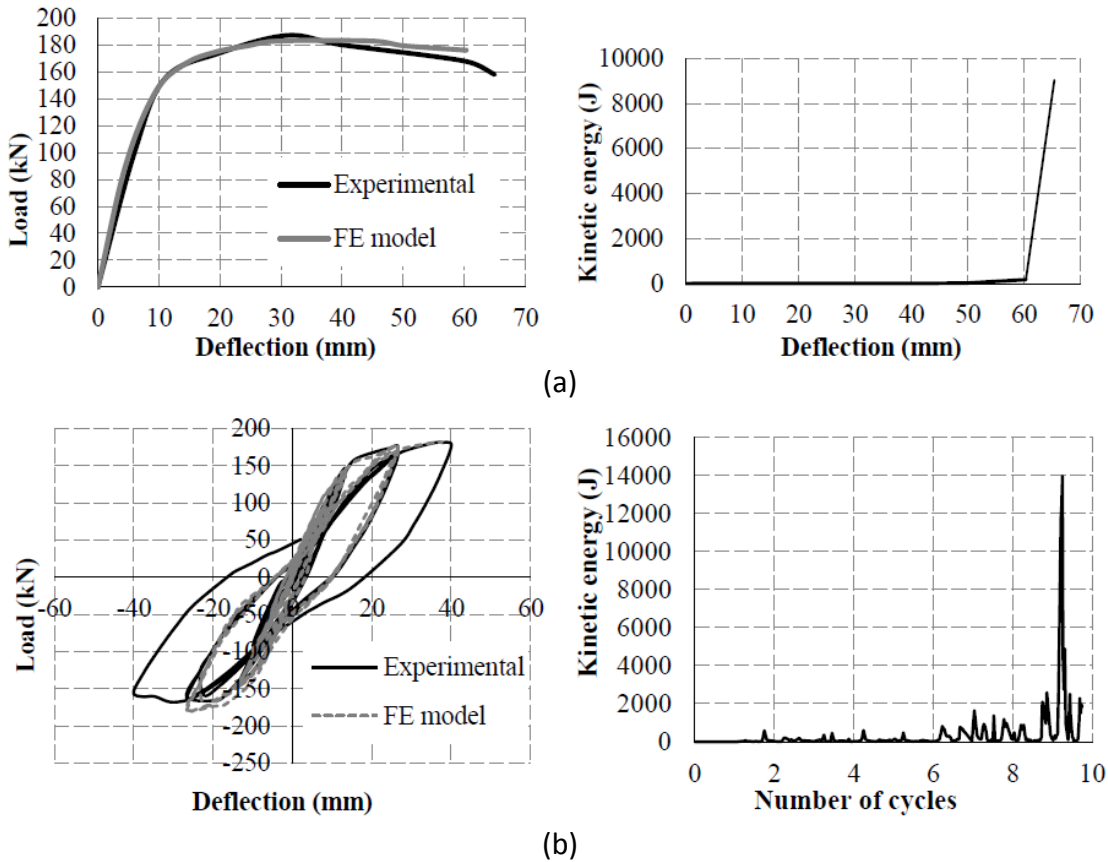


**Fig. 21:** Comparison between experimental and numerical results for statically-indeterminate columns Kotsovos *et al.* [45] under (a) monotonic and (b) cyclic loading, and corresponding kinetic energy profiles used to determine failure

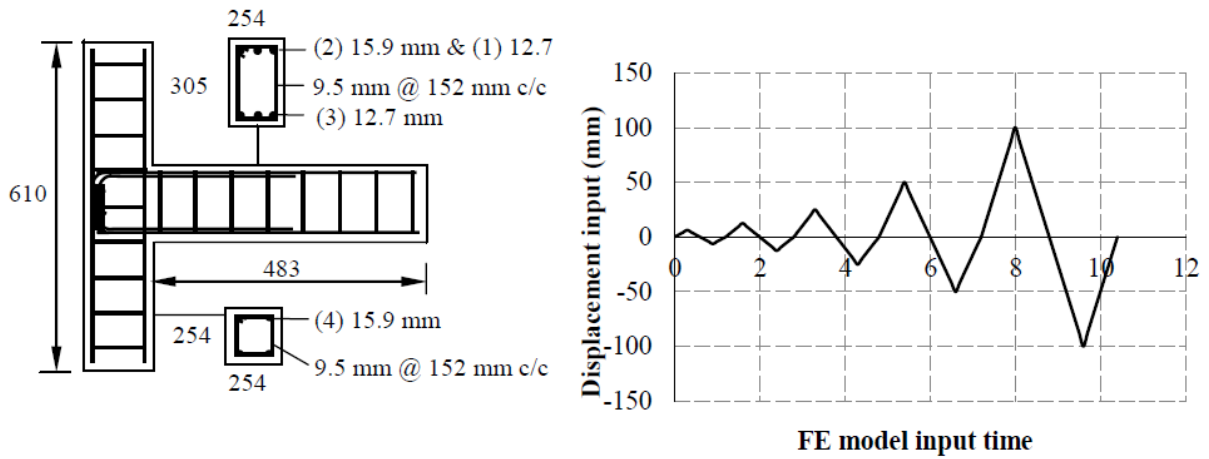
**10. SFRC beam-column joint sub-assemblages**

The applicability of the adopted FE model was also examined for more complex structural configurations such as SFRC beam-column joint sub-assemblages. The provision of steel fibres is particularly useful for seismic design as the detailing requirements in design codes of practice such as Eurocode 8 [46] often lead to congestion of traverse (i.e. hoop)

conventional reinforcement which can be challenging in construction terms. The fibres can potentially be used to partially replace some of the transverse reinforcement and hence relax the spacing between the conventional hoops. This was examined experimentally for both external (T) joints as well as internal (cross) joints by Bayasi and Gebman [47] and Filiatrault *et al.* [48], respectively. Both were tested under reversed-cyclic loads to mimic seismic action. The experimental studies were utilised for FE modelling validation purposes in the present study. Further FE-based parametric studies were carried out on both types of SFRC beam-column joints and the findings are discussed elsewhere [20].

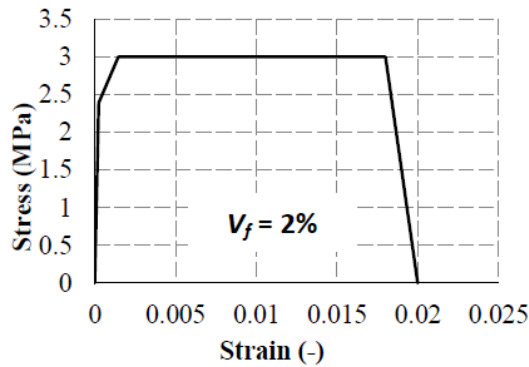
### 10.1. External (T) joint specimens

The geometry and reinforcement arrangements for the external beam-column joint tested by Bayasi and Gebman [47] are depicted in Fig. 22. The tensile stress-strain diagrams adopted for both SFRC and conventional steel reinforcement are also presented. The column was hinged at both ends whilst the reversed-cyclic load was applied vertically near the free-end of the cantilever beam using a displacement-based method for FE modelling purposes and the corresponding loading history is depicted in Fig. 22(a). A comparison between the ensuing load-deflection hysteresis loops based on both the experimental and numerical studies is presented in Fig. 23. The key characteristics of the curves are also summarised in a tabular form beneath the curves (these are the yield load  $P_y$  and corresponding deflection  $\delta_y$ , the maximum load and deflection  $P_{max}$  and  $\delta_{max}$ , the load and deflection at failure  $P_u$  and  $\delta_u$  and the ductility ratio  $\mu$  defined as  $\mu = \delta_u / \delta_y$ ). During the numerical investigation, failure (i.e. loss of load-carrying capacity) was associated with an abrupt large increase in kinetic energy as shown in Fig. 23, indicating the presence of large/extensive cracks within and around the joint region. The failure in the FE-based work was detected slightly earlier than the one found experimentally as the FE model was successful in simulating the experiments up to about four cycles before failure, compared to five cycles achieved experimentally. The comparison shows that all outputs including ductility levels were the same for the first four cycles, nevertheless the presence of the fifth cycle in the experimental data led to a discrepancy in the highest ductility value (with the FE predictions being on the safe side).

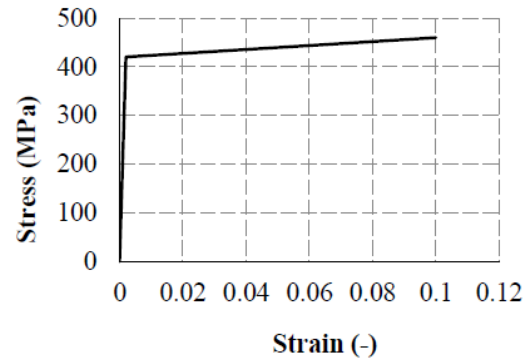


Fibre type	$L$ [mm]	$d$ [mm]	$V_f$ [%]	$f_c$ [MPa]
Hooked-end	30	0.5	2%	23.9

(a)

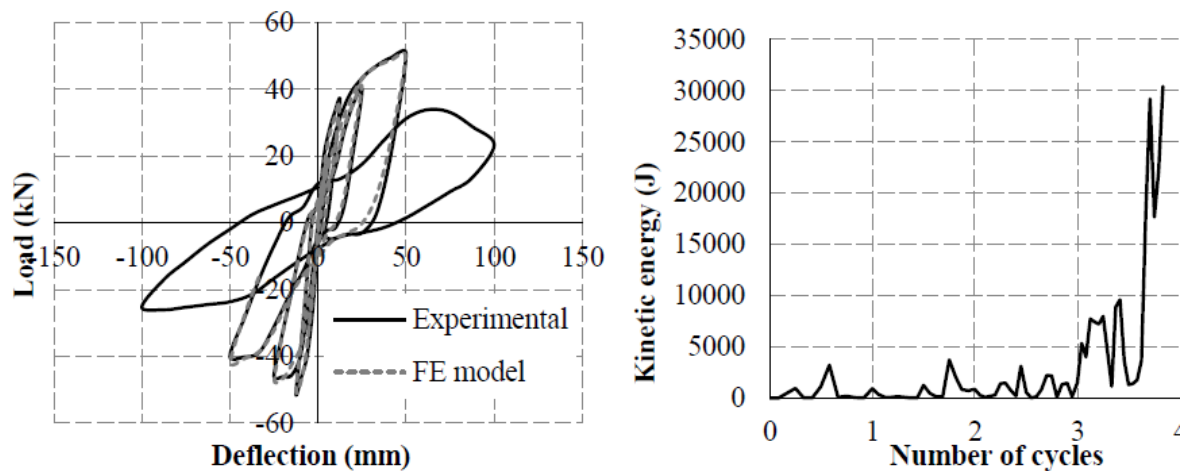


(b)



(c)

**Fig. 22:** Internal beam-column joints tested by Bayasi and Gebman [47]: (a) reinforcement, loading and material properties and tensile stress-strain diagram for (b) SFRC and (c) steel bars



	$P_v$ (kN)	$\delta_v$ (mm)	$P_u$ (kN)	$\delta_u$ (mm)	$P_{max}$ (kN)	$\delta_{max}$ (mm)	$\mu = \delta_u/\delta_v$	$P_{max}/P_v$
Experimental	18.5	6.25	23.3	100	50.9	50	16.0	2.75
FE model	19.3	6.25	50.0	49.6	50.0	49.6	7.94	2.59

**Fig. 23:** Comparison between experimental and numerical results obtained for internal joints tested Bayasi and Gebman [47] under cyclic loading and corresponding kinetic energy profiles used to determine failure

## 10.2. Internal (cross) joint specimens

The geometry and reinforcement details of the SFRC internal beam-column joint tested by Filiatrault *et al.* [48] are presented in Fig. 24. The specimen considered herein is the one referred to as S3 in Filiatrault *et al.* [48] original tests (three specimens were tested, one representing a joint with full seismic detailing at critical sections using a dense arrangement of conventional transverse hoop reinforcement and this was referred to as S2, whilst the spacing of the hoops was reduced in specimen S1 and then steel fibres were added in specimen S3 to examine whether or not the fibres can act as a replacement). For specimen S3, hooked-end steel fibres which were 50 mm in length and 0.5 mm in diameter were introduced in the critical region around the joint with  $V_f = 1.6\%$ . The compressive strength of concrete used was 46 MPa, modulus of elasticity was 35 GPa whilst the yield strength of steel bars was 400 MPa. The tensile stress-strain diagrams adopted for SFRCis depicted in Fig. 23(b), which also shows the displacement-based loading history for the cyclic load.

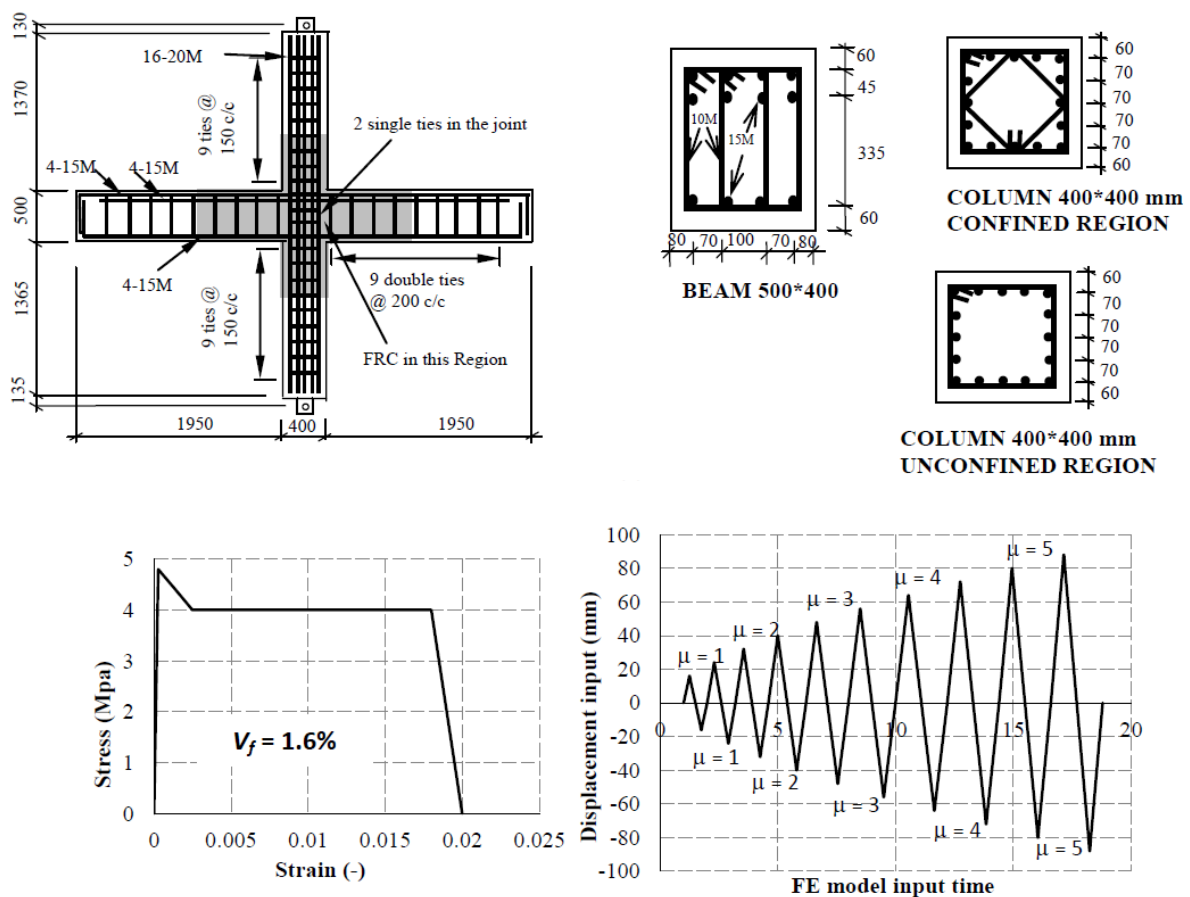
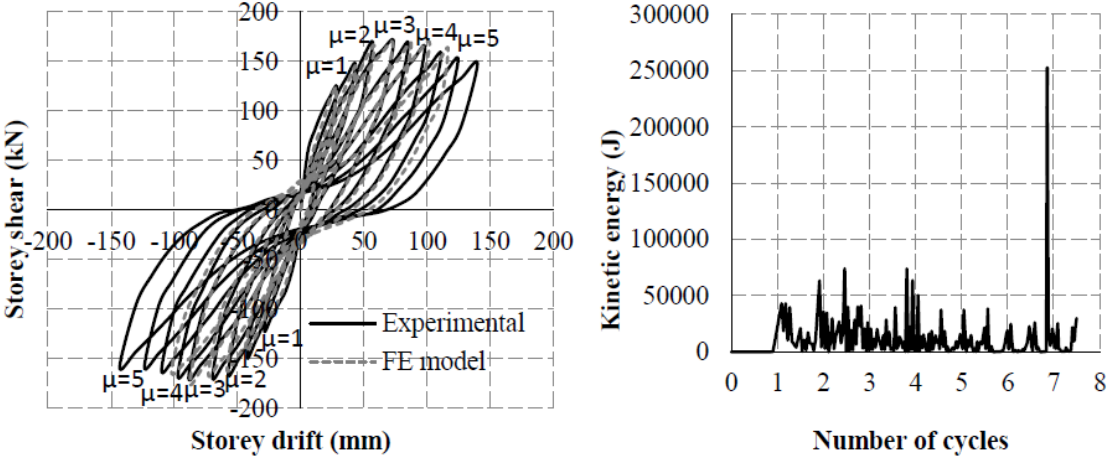


**Fig. 24** External beam-column joint tested by Filiatrault *et al.* [48]: (a) reinforcement details and (b) material properties and cyclic loading history

During testing both ends of the column were assumed to be simply-supported in order to simulate mid-storey inflection points. A constant axial compressive load of 670 kN was initially imposed onto the column representing gravity floor loads (for the prototype building considered) and the specimen was subsequently subjected to a reversed-cyclic loading applied on the beams to mimic seismic action. Fig. 25 shows a comparison between the experimental and FE-based hysteresis curves (which depict the relationship between storey shear and storey drift of the cross joint considered), with a table summarising key values also presented beneath the curves. Similarly to the preceding T-joint case, these include the yield, maximum and failure loads and corresponding displacement values as well as the ductility ratio. The energy-based failure criterion used for the numerical results is also shown.



	$P_y$ (kN)	$\delta_y$ (mm)	$P_{max}$ (kN)	$\delta_{max}$ (mm)	$P_u$ (kN)	$\delta_u$ (mm)	$\mu = \delta_u / \delta_y$	$P_{max} / P_y$
Experiment	123.9	28.7	170.1	73.6	140.0	147.9	5.15	1.37
FE model	122.4	28.6	168.0	102.2	162.7	116.8	4.08	1.37

**Fig. 25:** Comparison between experimental and numerical results obtained for external joints tested by Filiatrault *et al.* [48] under cyclic loading and corresponding kinetic energy profiles used to determine failure

The FE model was successful in simulating seven cycles compared to nine in the experimental work. The comparison of numerical and experimental results shows good agreement for the corresponding seven cycles. Even when considering the additional two cycles, the numerically-predicted values of storey shear  $P_y$  and  $P_{max}$  associated with yield and the maximum values are close to their experimental counterparts with a discrepancy of less than  $\sim 4\%$ . Nevertheless, the earlier failure prediction in the FE-based work led to the

ultimate (i.e. failure) displacements being ~20% less than the ultimate values established experimentally. These differences are well within the accepted range of accuracy for concrete structures, with the FE predictions being on the safe side. It has to be borne in mind that, as explained earlier, the latter was achieved due to the additional two experimental cycles, the results being similar within the first seven cycles. In addition, a distinction needs to be drawn between the definitions of failure in the numerical and experimental results. During testing, the loading procedure ended after the specimen suffered severe destruction of concrete within and around the joint region. On the other hand, in the numerical work the specimen was considered to have failed once a large sudden jump in the kinetic energy is detected as this is taken as an indication of severe cracking impairing the structural integrity of the joint (this is more stringent than simply considering the numerical failure due to the stiffness matrix becoming non-positive). During testing however, despite the destruction of concrete, the real structure may have still been capable of sustaining the induced excitation, by resorting briefly to alternative resistance mechanisms such as dowel action for instance. This is clearly neither stable nor sustainable and as such is of no real significance for design purposes (and as such the development of such *post-failure* mechanisms was not considered realistic in the FE work). Similarly to the experimental data, the numerical model was also successful in indicating the development of plastic hinges at the roots of the beams adjoining the columns and a reduction in cracking within the joint region due to the addition of steel fibres.

## **11. Conclusions**

In the present research work, an FE model for analysing SFRC is examined. Several structural arrangements and loading conditions were considered in order to assess the generality and objectivity of the proposed model and associated numerical strategy. Initially, SFRC small notched beam specimens were modelled in order to study the responses at the *material* level. Several sets of experimental data were considered and the comparisons with the numerical results have shown that the adopted FE model was successful in simulating these responses. The work was then extended to investigate the behaviour at the *structural* level and different SFRC structural forms were considered including simply-supported beams under monotonic and cyclic loading, statically-indeterminate columns under both axial and lateral monotonic and cyclic loading, external and internal joints under cyclic loading (the latter were applied in reversed cycles to mimic seismic action).

Based on the comparisons between the FE-based results and their experimental counterparts it was found that the model employed, despite its simplicity, is capable of providing realistic predictions of the key aspects of structural behaviour (i.e. load-bearing capacity, load-deflection curves, deformation profiles and modes of failure) for all cases of SFRC structural configurations presently considered. The brittle cracking model (provided in ABAQUS software) adopted in the present study focuses on the all-important fundamental parameters affecting concrete behaviour, namely brittleness and cracking both driven by tensile behaviour. Therefore, adequate description of the latter led to successful simulations of different SFRC structural forms and the fundamental nature of the brittle cracking model tempered the need for recalibration, which is often the drawback in more elaborate models limiting their generality. Even in instances when there was some difference between experiential and numerical results, the discrepancy was always on the safe side as the FE-based results did not over-estimate the actual strength values. Other models available in ABAQUS were considered as part of the present research project [12] and the best results were obtained from the brittle cracking model, confirming the ability of this model to efficiently capture the essential features of concrete behaviour. Furthermore, several constitutive models for SFRC were studied and subsequently the one proposed by Lok and Xiao [26] was selected and incorporated into the brittle cracking model in ABAQUS and it was found to yield predictions that are in good agreement with experimental data. This basic, yet profound and targeted approach, allows for the development of a fundamental understanding of the key aspects affecting the structural responses of SFRC structures.

## References

- [1] Cotsovos, D.M., 2004. *Numerical Modelling of Structural Concrete under Dynamic (Earthquake and Impact) Loading*, PhD Thesis, Imperial College London, London, UK.
- [2] Cotsovos, D.M., Zeris, C.A., Abbas, A.A., 2009. Finite element modelling of structural concrete, *Proceedings of the International Conference on Computational Methods in Structural Dynamics COMPDYN 2009*, Rhodes, 22-24 June 2009.
- [3] Kotsovos M.D., Pavlović M.N., Cotsovos D.M. 2008. Characteristic features of concrete behaviour: Implications for the development of an engineering finite-element tool, *Computers and Concrete*, 5(3), 243–260.

- [4] Kotsovos M.D. 1983. Effect of testing techniques on the post-ultimate behaviour of concrete in compression, *Materials and Structures*, RILEM, 16(91), 3–12.
- [5] Van Mier J. G.M. 1984. *Strain-softening of concrete under multiaxial loading conditions*, PhD thesis, Eindhoven University of Technology, Netherlands.
- [6] Van Mier J. G.M., Shah S.P., Armand M., Balayssac J.P., Bascoul A., Choi S., Dasenbrock D., Ferrara G., French C., Gobbi M.E., Karihaloo B.L., Konig G., Kotsovos M.D., Labuz J., Lange-Korbar D., Markeset G., Pavlović M.N., Simsch G., Thienel K-C., Turatsinze A., Ulmer M., Van Geel H. J. G. M., Van Vliet M. R.A., Zissopoulos D. 1997. Strain softening of concrete in uniaxial compression, *Materials and Structures*, RILEM, 30(4), 195–209.
- [7] Zissopoulos P.M., Kotsovos M.D., Pavlović M.N. 2000. Deformational behaviour of concrete specimens in uniaxial compression under different boundary conditions, *Cement and Concrete Research*, 30(1), 153–159.
- [8] Cotsovos D.M., Kotsovos M.D. 2011. Constitutive Modelling of Concrete Behaviour: Need for Reappraisal, *Computational Methods in Earthquake Engineering*, 21, 147–175.
- [9] Asteris P.G, Cotsovos D.M., Chrysostomou C.Z., Mohebkhah A., Al-Chaar G.K. 2013. Mathematical Micromodeling of Infilled Frames: State of the Art, *Engineering Structures*, 56, 1905–1921.
- [10] Kotsovos, M.D., Pavlović, M.N., 1995. *Structural concrete, Finite-element analysis for limit-state design*, Thomas Telford, London, UK.
- [11] ABAQUS Version 6.7 Documentation, 2007. Available online at <http://www.simulia.com/services/training/V67-Introduction-DEMO/AbaqusV67Intro.htm> (accessed 12/03/2015).
- [12] Kotsovos, G.M., 2011 Assessment of the flexural capacity of RC beam/column elements allowing for 3d effects. *Engineering Structures*, 33(10), 2772–2780
- [13] Kotsovos, M.D., 2014 *Compressive Force-Path Method-Unified Ultimate Limit-State Design of Concrete Structures*. Springer Cham Heidelberg New York Dordrecht London.
- [14] Syed Mohsin, S.M., 2012. *Behaviour of fibre-reinforced concrete structures under seismic loading*, PhD thesis, Imperial College London, London, UK.
- [15] Abbas, A.A., Syed Mohsin, S.M. and Cotsovos, D.M., 2010. Numerical modelling of fibre-reinforced concrete, *Proceedings of the International Conference on Computing*

- in Civil and Building Engineering icccbe 2010*, W.Tizani, ed, Nottingham, UK, June-July2010, Paper 237, p. 473, University of Nottingham Press, ISBN 978-1-907284-60-1.
- [16] Abbas, A.A., Syed Mohsin, S.M. and Cotsovos, D.M., 2010. A comparative study on modelling approaches for fibre-reinforced concrete, *Proceedings of the 9<sup>th</sup> HSTAM International Congress on Mechanics*. Limassol, Cyprus, July 2010.
- [17] Abbas, A A, Syed Mohsin, S, Cotsovos, D M, Ruiz-Teran, A M, 2014. Shear behaviour of SFRC simply-supported beams, *ICE Proc. Structures and Buildings*, 167(SB9), 544–558.
- [18] Abbas, A.A., Syed Mohsin, S.M., Cotsovos, D.M. and Ruiz-Teran, A.M., 2014. Nonlinear analysis of statically-indeterminate SFRC columns, *Structural Concrete*, 15(1), 94–105.
- [19] Abbas, A A, Syed Mohsin, S, Cotsovos, D M, Ruiz-Teran, A M, 2014. Statically-indeterminate SFRC columns under cyclic loads, *Advances in Structural Engineering*, 17(10), 1403–1417.
- [20] Abbas, A.A., Syed Mohsin, S.M., Cotsovos, D.M. and Ruiz-Teran, A.M., 2014. Seismic response of steel fibre reinforced concrete beam–column joints, *Engineering Structures*, 59, 261–283.
- [21] RILEM Technical Committees, 2000. RILEM TC 162-TDF: Test and Design Methods for Steel Fibre-Reinforced Concrete, Recommendation:  $\sigma - \epsilon$ Design Method, *Materials and Structures*, RILEM, 33(2), 75–81.
- [22] RILEM Technical Committees, 2003. RILEM TC 162-TDFa: Test and Design Methods for Steel Fibre-Reinforced Concrete, Final Recommendation:  $\sigma - \epsilon$ Design Method, *Materials and Structures*, RILEM, 36(8), 560–567.
- [23] Barros, J.A.O. and Figueiras, J.A., 1999. Flexural behavior of SFRC: Testing and modelling. *Journal of Materials in Civil Engineering*, ASCE, 11(4), 331 – 339.
- [24] Barros, J.A.O. and Figueiras, J.A., 2001. Model for the Analysis of Steel Fibre Reinforced Concrete Slabs on Grade. *Computers and Structures*, 79, 97 – 106.
- [25] Tlematb, H., Pilakoutas, K. and Neocleous, K., 2006. Modelling of SFRC using Inverse Finite Element Analysis, *Materials and Structures*, RILEM, 39, 221–233.
- [26] Lok, T.S. and Xiao, J.R., 1999. Flexural Strength Assessment of Steel Fibre-Reinforced Concrete, *Journal of Materials in Civil Engineering*, ASCE, 11(3), 188 – 196.

- [27] Lok, T.S. and Pei, J.S., 1996. Flexural Behavior of Steel Fibre-Reinforced Concrete, *Journal of Materials in Civil Engineering*, ASCE, 10(2), 86 – 97.
- [28] National Research Council, 2007. *Guide for the Design and Construction of Fibre-Reinforced Concrete Structures*. CNR-DT 204/2006.
- [29] RILEM Technical Committees, 2002. RILEM TC 162-TDF: Test and Design Methods for Steel Fibre-Reinforced Concrete, Design of Steel Fibre-Reinforced Concrete using the  $\sigma - w$  Method: Principles and Application, *Materials and Structures*, RILEM, 35(249), 262-278.
- [30] Cho, S.H. and Kim, Y.I., 2003. Effects Steel Fibres on Short Beams Loaded in Shear, *ACI Structural Journal*, 100(79), 765 – 774.
- [31] Campione, G. and Mangiavillano, M.L., 2008. Fibrous reinforced concrete beams in flexure: Experimental investigation, analytical modelling and design considerations. *Engineering Structures*, 30, 2970 – 2980.
- [32] Bencardino, F., Rizzuti, L., Spadea, G., and Ramnath, N.S., 2008. Stress-Strain Behavior of Steel Fibre-Reinforced Concrete in Compression. *Journal of Materials in Civil Engineering*, ASCE, 20(3), 255 – 262.
- [33] Sharma, A.K., 1986. Shear Strength of Steel Fibre Reinforced Concrete Beams. *ACI Journal*, 83(4), 624 – 628.
- [34] Mansur, M.A. and Ong, K.C.G., 1991. Behaviour of Reinforced Concrete Deep Beams in Shear. *ACI Structural Journal*, 88, 98 – 105.
- [35] Oh, B.H., Lim, D.H., Yoo, S.W. and Kim, E.S., 1998. Shear behaviour and shear analysis of reinforced concrete beams containing steel fibres. *Magazine of Concrete Research*, 50(4), 283–291.
- [36] Kwak, Y.K, Eberhard, M.O, Kim, W.S. and Kim, J., 2002. Shear Strength of Steel Fibre-Reinforced Concrete Beams without Stirrups. *ACI Structural Journal*, Technical Paper, No. 99-S55; 530 – 538.
- [37] Campione, G., La Mendola, L., Papia, M. (2006). “Shear strength of steel fibre reinforced concrete beams with stirrups”, *Structural Engineering and Mechanics*, 24(1), 107-136.
- [38] Zienkiewicz, O.C. and Taylor, R.L., 2005. *Vol. 2: The Finite Element Method for Solid and Structural Mechanics*, 6<sup>th</sup> edition, Butterworth-Heinemann, Oxford, UK.
- [39] Cook, R.D., 1995. *Finite element modelling for stress analysis*, John Wiley & Sons, USA.

- [40] Zheng, Y., Robinson, D., Taylor, S. and Cleland, D., 2012. Non-linear finite-element analysis of punching capacities of steel–concrete bridge deck slabs. *Structures and Buildings, ICE Proceedings* 165(5), 255–259.
- [41] Hughes, G. and Spiers, D.M., 1982. *An Investigation on the Beam Impact Problem*. Technical Report 546, Cement and Concrete Association, UK.
- [42] Bresler, G. and Scordelis, A.C., 1963. Shear Strength of Reinforced Concrete Beams, *ACI Journal*, 60(1), 51–74.
- [43] Barros, J.A.O., Cunha, V.M.C.F., Ribeiro, A.F. and Antune, J.A.B., 2005. Post-Cracking Behaviour of Steel Fibre-Reinforced Concrete, *Materials and Structures, RILEM*, 38, 47-56.
- [44] Trottier, J.F., and Banthia, N., 1994. Toughness Characterization of Steel Fibre-Reinforced Concrete, *Journal of Materials in Civil Engineering, ASCE*, 6(2), 264 – 289.
- [45] Kotsovos, G., Zeris, C., and Kotsovos, M., 2007. The Effect of Steel Fibres on the Earthquake-Resistance Design of Reinforced Concrete Structures, *Materials and Structures, RILEM*, 40, 175-188.
- [46] British Standard Institution, 2004. *BS EN 1998-1 Eurocode 8: Design of Structures for Earthquake Resistance – Part 1: General Rules, Seismic Actions and Rules for Buildings*, European Committee for Standardization, Brussels.
- [47] Bayasi, Z., and Gebman, M., 2002. Reduction of Lateral Reinforcement in Seismic Beam-Column Connection via Application of Steel Fibres, *ACI Structural Journal*, (99)6, 772–780.
- [48] Filiatrault, A., Pineau, S., and Houde, J., 1995. Seismic Behaviour of Steel Fibre-Reinforced Concrete Interior Beam-Column Joints, *ACI Structural Journal*, 543–552.
- [49] Ha, S.K., Jin, K.K. and Huang, Y. (2008). Micro-Mechanics of Failure (MMF) for Continuous Fibre Reinforced Composites, *Journal of Composite Materials*, 42(18): 1873–1895.